

HyperInterval: Hypernetwork Approach to Training Weight Interval Regions in Continual Learning

Patryk Krukowski^{1,2}, Anna Bielawska², Kamil Książek² Paweł Wawrzynski¹ Paweł Batorski²
Przemysław Spurek^{1,2}

¹IDEAS NCBR

²Jagiellonian University

{patryk.krukowski,pawel.wawrzynski}@ideas-ncbr.pl, {kamil.ksiazek,przemyslaw.spurek}@uj.edu.pl,
annabielawska07@gmail.com, pawel.batorski@doctoral.uj.edu.pl

Abstract

Recently, a new Continual Learning (CL) paradigm was presented to control catastrophic forgetting, called Interval Continual Learning (InterContiNet), which relies on enforcing interval constraints on the neural network parameter space. Unfortunately, InterContiNet training is challenging due to the high dimensionality of the weight space, making intervals difficult to manage. To address this issue, we introduce HyperInterval, a technique that employs interval arithmetic within the embedding space and utilizes a hypernetwork to map these intervals to the target network parameter space. We train interval embeddings for consecutive tasks and train a hypernetwork to transform these embeddings into weights of the target network. An embedding for a given task is trained along with the hypernetwork, preserving the response of the target network for the previous task embeddings. Interval arithmetic works with a more manageable, lower-dimensional embedding space rather than directly preparing intervals in a high-dimensional weight space. Our model allows faster and more efficient training. Furthermore, HyperInterval maintains the guarantee of not forgetting. At the end of training, we can choose one universal embedding to produce a single network dedicated to all tasks. In such a framework, hypernetwork is used only for training and, finally, we can utilize one set of weights. HyperInterval obtains significantly better results than InterContiNet and gives SOTA results on several benchmarks.

1 Introduction

Humans have a natural ability to learn from a continuous flow of data, as real-world data is usually presented sequentially. Humans need to be able to learn new tasks while also retaining and utilizing knowledge from previous tasks. While deep learning models have achieved significant success in many individual tasks, they struggle in this aspect and often perform poorly on the preceding tasks after learning new ones, which is known as catastrophic forgetting (McCloskey and Cohen 1989; Ratcliff 1990; French 1999).

Continual learning (CL) is an important area of machine learning that aims to bridge the gap between human and machine intelligence. While several methods have been proposed to effectively reduce forgetting when learning new tasks, such as that by Kirkpatrick et al. (2017); Lopez-Paz and Ranzato (2017); Shin et al. (2017); Aljundi et al. (2018); Masse, Grant, and Freedman (2018); Rolnick et al. (2019);

van de Ven, Siegelmann, and Tolias (2020), they typically do not provide any solid guarantees about the extent to which the model experiences forgetting.

In the Interval Continual Learning (InterContiNet) (Wołczyk et al. 2022), authors propose a new paradigm that uses interval arithmetic in CL scenarios. The main idea is to use intervals to control weights dedicated to subsequent tasks. Thanks to strict interval arithmetic, these authors can enforce a network to give the same prediction for each weight sampled from the interval. Moreover, they can force the interval of the new task to be entirely contained in the hyperrectangles of the previous ones. The two above properties allow one to obtain strict constraints for forgetting. The model has strong theoretical fundamentals and obtains good results in incremental tasks and domain scenarios on relatively small datasets. The main limitation of InterContiNet is a complicated training process. To allow for the training of new tasks, one has to use large intervals in the weight space, which is trained in an extremely high-dimensional parameter space. Consequently, the model is limited to simple architectures, datasets, and continuous learning scenarios.

To solve such a problem, we propose HyperInterval¹, i.e. a model which uses intervals in the embedding space and a hypernetwork to transfer them to the weight space of the target network, see Fig. 1. Such a solution allows one to effectively train interval-based target network on large datasets and the most difficult incremental class scenarios, surpassing its foregoing limitations. A hypernetwork architecture (Ha, Dai, and Le 2016) is defined as a neural network that generates weights for a specific target network designed to solve a particular problem. In continual learning, a hypernetwork may generate weights for the target model (von Oswald et al. 2019; Henning et al. 2021; Książek and Spurek 2023). Dependent on the task identity, trainable embeddings are fed into the hypernetwork. After training is complete, a single meta-model can create task-specific weights. This ability to generate distinct weights for various tasks enables models based on hypernetworks to maintain minimal knowledge loss.

In HyperInterval, we use interval arithmetic in an embedding space. The hypernetwork is fed with task specific in-

¹The source code is available at <https://github.com/gmum/HyperInterval>

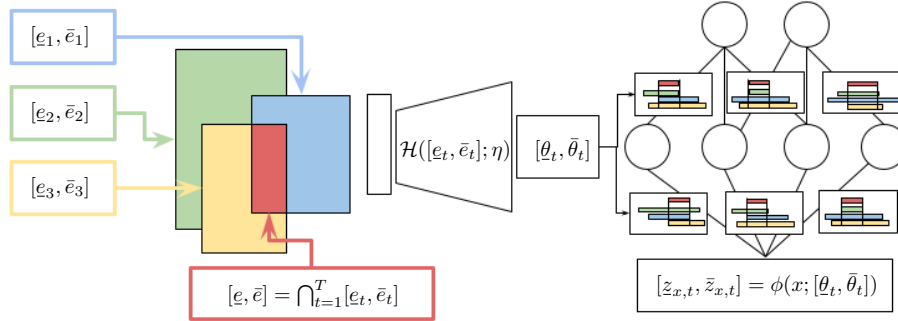


Figure 1: HyperInterval uses interval arithmetic in the input to the hypernetwork. After propagating the intervals through the hypernetwork, we obtain the intervals on the target network layers. The intersection of all intervals produces universal embeddings dedicated to all tasks. Our model gives theoretical guarantees for not forgetting.

interval embedding to produce weights for the target network. Our architecture uses a target model with interval weights and Interval Bound Propagation (IBP) (Gowal et al. 2018) technique in the hypernetwork. Due to low dimension of the task embeddings, this solution provides greater robustness to forgetting than previous approaches to CL based on interval arithmetic.

Our model can be used in incremental class learning in both scenarios: with and without task identity. We can use the evaluation scenario proposed by hypernetwork-based models (von Oswald et al. 2019; Henning et al. 2021; Książek and Spurek 2023). For known task identity scenarios, we use interval arithmetic as a regularization technique, and each task embedding produces new target network interval weights dedicated to this task. We can also use an entropy criterion to determine a class identity when it is unknown. In both solutions, we must memorize hypernetwork and all task embeddings. Our framework allows us to produce a universal embedding. With interval arithmetic, we can control intervals and transform them into interval embeddings with non-empty intersections. At the end of the training, we generate the final target network from the universal embedding created from the intersection of all previously trained interval embeddings, being able to solve all tasks. Such an approach significantly outperforms InterContiNet and in many cases outperforms state-of-the-art methods.

Our contributions can be summarized as follows:

- We show HyperInterval, which uses interval arithmetic in the embedding space and a hypernetwork to propagate intervals to the target network weight space.
- We demonstrate that our model can efficiently use interval arithmetic in CL settings in incremental class learning scenarios with large datasets.
- We demonstrate that a hypernetwork can be used to recursively refine, across consecutive tasks, the region of target network weights that are universally effective for all tasks.

2 Related Works

Continual learning. When a neural network is trained on new data, it often forgets patterns learned from previous data, a problem known as *catastrophic forgetting* (French 1999). Continual learning methods enable the network to learn new tasks without losing performance on earlier ones, even when previous data is no longer available. Different setups exist for continual learning (van de Ven and Tolias 2019): in task-incremental learning, the task is known during inference; in class-incremental learning, the network must learn a consistent input-output distribution across tasks with varying data distributions.

Rehearsal methods store a limited-size representation of previous tasks and train the network on a combination of data samples from the previous and current tasks. In the simplest setup, a memory buffer is used to store selected previous samples in their raw form (Lopez-Paz and Ranzato 2017; Aljundi et al. 2019; Prabhu, Torr, and Dokania 2020) or store exemplars of classes in the class incremental setting (Rebuffi et al. 2017; Chaudhry et al. 2018; Castro et al. 2018; Wu et al. 2019; Hou et al. 2019; Belouadah and Popescu 2019). Some methods instead of using raw data samples, store data representations of previous tasks in different forms, e.g., optimized artificial samples (Liu et al. 2020), distilled datasets (Wang et al. 2018; Zhao, Mopuri, and Bilen 2021) or addressable memory structures (Deng and Russakovsky 2022).

Buffer-based approaches raise questions of scalability and data privacy. To address these questions, generative rehearsal methods are based on generative models that produce data samples similar to those present in previous tasks, instead of just replaying them from a storage. In Deep Generative Replay (Shin et al. 2017), a Generative Adversarial Network (GAN) is used as a model to generate data from the previous tasks. For the same purpose, Variational Autoencoders (VAE) are used in (van de Ven and Tolias 2018), Normalizing Flows in (Nguyen et al. 2018), Gaussian Mixture Models in (Rostami, Kolouri, and Pilly 2019) and Diffusion Models in (Cywiński et al. 2024).

Regularization methods (Kirkpatrick et al. 2017; Zenke,

Poole, and Ganguli 2017; Li and Hoiem 2017) are designed especially for the task incremental setup. They identify neural weights with the greatest impact on task performance and slow down their learning on further tasks through regularization.

Architectural methods (Rusu et al. 2016; Yoon et al. 2018; Mallya and Lazebnik 2018; Mallya, Davis, and Lazebnik 2018; Wortsman et al. 2020) are especially designed for the task incremental setup. They adjust the structure of the model for each task.

Wolczyk et al. (2022) introduced the InterContiNet algorithm. For each task, this method identifies a region in the weight space in which any weight vector assures a good performance. A weight vector proper for all tasks is taken from the intersection of these regions. In InterContiNet, these regions take the form of hyperrectangles. The training of InterContiNet in a continual learning setting is problematic since intervals in the high-dimensional parameter space need to be controlled. To alleviate these problems, the authors engineered an elaborate training procedure. However, in a multidimensional weight space, it is difficult to optimize weight hyperrectangles for different tasks to have a non-empty intersection. Consequently, InterContiNet is limited to relatively simple architectures, datasets, and CL scenarios. In (Henning et al. 2021), the regions in the weight space take the form of normal distributions. In the architecture presented there, a hyper-hypernetwork transforms inputs into task-specific embeddings which a hypernetwork transforms into those distributions in the weight space of the target network. The current work develops the same emerging family of methods that could be called regional methods. However, here we consider regions that result from the transformation of low-dimensional cuboids assigned to tasks by a hypernetwork. This way, we overcome the issue of scalability and present an architecture capable of dealing with complex architectures, datasets and CL scenarios.

3 Method: HyperInterval

Our proposed CL architecture, dubbed HyperInterval, is presented in Fig. 1, and based on the following logic. Hyperrectangular, learnable task embeddings are fed to the hypernetwork, which produces weights for the target network, which solves the CL task. Both networks use the interval arithmetic. The intersection of all task interval embeddings forms a universal interval embedding, from which every embedding is suitable for all CL tasks. The training procedure preserves the performance of the architecture on previous tasks. Below, we present separate parts of this architecture. We commence with a presentation of the target network and the principles of interval neural networks, and then we describe the interval hypernetwork.

3.1 Interval target network

In interval neural networks, (Dahlquist and Björck 2008, Sec. 2.5.3, Wolczyk et al. 2022) instead of considering particular points $\vartheta \in \mathbb{R}^D$ in the parameter space, regions $\Theta \subset \mathbb{R}^D$ are used. The hyperrectangle $[\underline{\theta}, \bar{\theta}]$ is a Cartesian

product of one-dimensional intervals

$$[\underline{\theta}, \bar{\theta}] = [\underline{\theta}^{(1)}, \bar{\theta}^{(1)}] \times [\underline{\theta}^{(2)}, \bar{\theta}^{(2)}] \times \dots \times [\underline{\theta}^{(D)}, \bar{\theta}^{(D)}] \subset \mathbb{R}^D,$$

where by $\theta^{(i)} \in [\underline{\theta}^{(i)}, \bar{\theta}^{(i)}]$ we denote the i -th element of θ . Interval arithmetic utilizes operations on segments. By $\phi(x; \theta)$ we denote the target network, which is a layered neural classifier with input x and weights θ . We assume the weights θ to be intervals, thus altogether define a hyperrectangle, $[\underline{\theta}, \bar{\theta}]$. Therefore, for a given input x , the network produces a hyperrectangular output $[\underline{z}, \bar{z}] = \phi(x; [\underline{\theta}, \bar{\theta}])$, rather than a vector. Appendix A provides details of the interval network inner workings.

Since intervals are used instead of points, the worst-case cross-entropy is used instead of classical ones. The worst-case interval-based loss is defined by

$$\hat{\ell}(x, y; [\underline{\theta}, \bar{\theta}]) = \ell(\hat{z}, y), \quad (1)$$

where x is an observation, y is an one-hot encoded class of x , $\ell(\cdot, \cdot)$ is the cross-entropy loss, and \hat{z} is a vector with the i -th element defined as:

$$\hat{z}^{(i)} = \begin{cases} \bar{z}^{(i)}, & \text{for } y^{(i)} = 0, \\ \underline{z}^{(i)}, & \text{for } y^{(i)} = 1, \end{cases}$$

where $z = \phi(x; [\underline{\theta}, \bar{\theta}])$. The worst-case cross-entropy, as shown in (Wolczyk et al. 2022, Theorem 3.1), gives a strict upper limit on cross-entropy

$$\hat{\ell}(x, y; [\underline{\theta}, \bar{\theta}]) \geq \max_{\theta \in [\underline{\theta}, \bar{\theta}]} \ell(\phi(x; [\theta, \theta]), y). \quad (2)$$

For the continual learning challenge of optimizing across the tasks $1, \dots, T$, during the training on a specific task t , the goal is to achieve the optimal worst-case cross-entropy within the intervals $[\underline{\theta}_t, \bar{\theta}_t]$ where $[\underline{\theta}_t, \bar{\theta}_t] \subseteq [\underline{\theta}_{t-1}, \bar{\theta}_{t-1}]$. Interval arithmetic facilitates non-forgetting by maintaining the weights interval of task t within the weights interval trained for task $t - 1$.

Technically, the interval classifier ϕ employs for task t the parameter of the network with the central point θ_t and an interval radius $\varepsilon_t \in \mathbb{R}^D$. Therefore, the parameter region is defined as $[\underline{\theta}_t, \bar{\theta}_t] = [\theta_t - \varepsilon_t, \theta_t + \varepsilon_t]$. With this approach, the network can still function as a conventional non-interval model by using only the central weights θ_t , which consequently generates only the central activations for each layer. Concurrently, the activation intervals $[\underline{z}_l, \bar{z}_l]$ can be computed with interval arithmetic. As detailed by Goyal et al. (2018), these processes can be efficiently implemented on GPUs by simultaneously computing the central activations and their corresponding radii. The interval neural network redesigns the fundamental components of neural networks (such as fully-connected or convolutional layers, activations, and pooling) to accommodate interval inputs and weights.

3.2 Interval hypernetwork

In this section, we introduce a hypernetwork that transforms hyperrectangles in a low-dimensional embedding space into regions in the weight space of the target network. We demonstrate the effectiveness of this joint architecture. Finally, we show that the hypernetwork may be used only

in training, while during inference only the target network is utilized. A region in the target network weight space is shaped for all CL tasks iteratively, i.e. new constraints are defined for subsequent tasks. Finally, we can create a universal region of weights with a universal embedding vector. Still, we can produce weights for each task with dedicated embeddings, ensuring higher performance for individual tasks, but at the expense of less universality.

HyperInterval consists of the interval hypernetwork directly preparing weights for the interval target network which finally performs a classification. The consecutive parts of the HyperInterval architecture will be described in the next few paragraphs.

Hypernetwork Introduced in (Ha, Dai, and Le 2016), hypernetworks are neural models that produce weights for a distinct target network designed for solving a specific problem. Hypernetworks were already used in continual learning (von Oswald et al. 2019; Henning et al. 2021; Książek and Spurek 2023). In this context, they generate unique weights for individual CL tasks.

HNET (von Oswald et al. 2019) introduces trainable embeddings $e_t \in \mathbb{R}^M$, one for each task t , where $t \in \{1, \dots, T\}$. The hypernetwork, denoted as \mathcal{H} , and parameterized by η , outputs the weights specific to the t -th task, θ_t , for the target network ϕ , as shown in the equation: $\mathcal{H}(e_t; \eta) = \theta_t$.

The function $\phi(\cdot; \theta_t) : X \rightarrow Y$ represents a neural network classifier with weights θ_t generated by the hypernetwork $\mathcal{H}(\cdot; \eta)$ with weights η , and assigns labels for samples in a given task. Notably, the target network itself is not trained directly. Within HNET, a hypernetwork $\mathcal{H}(\cdot; \eta) : \mathbb{R}^M \ni e_t \mapsto \theta_t$ computes the weights θ_t for the target network ϕ based on the dedicated task embedding e_t . Consequently, each task in continual learning is represented by a classifier function $\phi(\cdot; \theta_t) = \phi(\cdot; \mathcal{H}(e_t; \eta))$.

After training, a single meta-model is produced, which furnishes weights for specific tasks. The capacity to generate distinct weights for each task allows hypernetwork-based models to exhibit minimal catastrophic forgetting. When learning the following task, essentially a new architecture is created, with weights dedicated to this task. To identify weights fitting to all tasks, we introduce HyperInterval, which uses a hypernetwork with interval arithmetic and, optionally, also training rules ensuring a joint weight subregion for more CL tasks. Basically, this scenario corresponds to a single architecture for a higher number of tasks. After training, we propagate the intersection of intervals through the hypernetwork to produce universal weights for all tasks. In such a scenario, we do not need to memorize embeddings and hypernetworks since one network is dedicated to all tasks.

Interval arithmetic in the embedding space. In HNET (von Oswald et al. 2019) and HNET-based models (Henning et al. 2021; Książek and Spurek 2023) authors use one-dimensional trainable embeddings $e_t \in \mathbb{R}^M$ for each task t , where $t \in \{1, \dots, T\}$. In HyperInterval, we use interval arithmetic, which results in an embedding defined by its lower and upper bound for each coordinate: $[\underline{e}_t, \bar{e}_t] = [e_t - \varepsilon_{t,i}, e_t + \varepsilon_{t,i}] = [e_t^{(1)} - \varepsilon_{t,i}^{(1)}, e_t^{(1)} +$

$\varepsilon_{t,i}^{(1)}] \times \dots \times [e_t^{(M)} - \varepsilon_{t,i}^{(M)}, e_t^{(M)} + \varepsilon_{t,i}^{(M)}] \subset \mathbb{R}^M$, where $\varepsilon_t = [\varepsilon_{t,i}^{(1)}, \dots, \varepsilon_{t,i}^{(M)}]$ is a perturbation vector during the i -th iteration of training the t -th task ($i \in \{1, \dots, n\}$) satisfying the condition $\sigma(\varepsilon_t) = 1$, where $\sigma(\cdot)$ is the softmax function. It is worth noting that such a normalization technique is applied to perturbed vectors before passing through the hypernetwork. Consequently, e_t denotes the center of the embedding for the t -th task. The presented condition ensures that intervals do not collapse to zero widths in training. Perturbation vector coordinates values are trainable when we create specific weights for each task or are strictly given in cases where we define a joint weight subregion for all tasks. Nevertheless, its values must be non-negative, i.e., $\varepsilon_{t,i}^j \geq 0$ for $j \in \{1, \dots, M\}$.

Thanks to using interval-based embeddings, we can select an embedding subspace to create regions dedicated to more CL tasks, see Fig. 1. In HyperInterval, interval embeddings are transformed by the hypernetwork into hyperrectangles of weights of the target model. In this scenario, the hypernetwork propagates segments instead of points. To achieve this, in the hypernetwork model, we use an architecture based on Interval Bound Propagation (IBP) (Gowal et al. 2018).

In our proposed HyperInterval, we use a hypernetwork whose weights η are vectors, but we propagate an interval input $[\underline{e}_t, \bar{e}_t]$ producing an interval output, i.e.,

$$[\underline{\theta}_t, \bar{\theta}_t] = \mathcal{H}([\underline{e}_t, \bar{e}_t]; \eta).$$

The inner workings of the hypernetwork are based on interval arithmetic. We elaborate more on this in Appendix B.

The hypernetwork \mathcal{H} is trained using the procedure described below. It is necessary to ensure that in learning a given task, HyperInterval does not forget the previously learned knowledge. Outputs from task-conditioned hypernetworks are generated based on the task embedding. To prevent the hypernetwork from forgetting previous tasks, we regularize its training to produce the same target network weights for previous task embeddings. In a training of task T with HyperInterval, the regularization loss is specified as:

$$\mathcal{L}_{output}(\eta) = \frac{1}{3(T-1)} \sum_{t=1}^{T-1} \sum_{\mu \in \{e_t, \frac{e_t + \bar{e}_t}{2}, \bar{e}_t\}} \|\mathcal{H}(\mu; \eta_{T-1}) - \mathcal{H}(\mu; \eta)\|^2,$$

where η_{T-1} are the hypernetwork weights trained for task $T-1$. The second component of the nested sum above corresponds to the regularization of the embedding center, i.e. $e_t = (\underline{e}_t + \bar{e}_t)/2$. The motivation for using this regularization formula is its ability to effectively preserve the knowledge acquired from previous tasks by controlling the interval lengths produced by the hypernetwork. Specifically, when the product of the hypernetwork's weights is small, the resulting intervals tend to be short. This outcome is a direct consequence of the Lipschitz continuity of MLP networks, which we use exclusively as hypernetworks. This made additional regularization redundant. For further validation, please refer to Appendix H.2.

The proposition and the proof of the Lipschitz continuity of MLP networks is detailed in Appendix D. Consequently, regularizing the endpoints of the intervals alone is

sufficient to maintain the knowledge from previous tasks. This conclusion is further supported by the fact that the proposed regularization imposes a non-increasing constraint on the interval. As a result, it is unnecessary to consider other points within the interval $[\underline{e}_t, \bar{e}_t]$ for regularization purposes. Nonetheless, we also apply additional regularization to the center of the interval, as this approach has been observed to yield slightly better results. When the task identity is given in the inference stage, then one can just use

$$\mathcal{L}_{output}(\eta) = \frac{1}{T-1} \sum_{t=1}^{T-1} \|\mathcal{H}(e_t; \eta_{T-1}) - \mathcal{H}(e_t; \eta)\|^2,$$

as we do not have to regularize the hypernetwork beyond the middle of the interval. The ultimate cost function is a sum of a component $\mathcal{L}_{current}$, defined by the current task data, and output regularization \mathcal{L}_{output} , i.e.,

$$\mathcal{L} = \mathcal{L}_{current} + \beta \cdot \mathcal{L}_{output}, \quad (3)$$

where β represents a hyperparameter managing the intensity of regularization. For an input-output data pair, (x, y) , the current loss is defined as the standard cross-entropy combined with the worst-case cross-entropy, i.e.,

$$\ell_{current} = \kappa \cdot \ell\left(\frac{z_L + \bar{z}_L}{2}, y\right) + (1 - \kappa) \cdot \ell(\hat{z}_L, y),$$

where κ is a hyperparameter scheduled during training helping to control the proper classification of samples. $\mathcal{L}_{current}$ in (3) is the average of $\ell_{current}$ over the current task data D_t .

Both components of \mathcal{L} are essential because HyperInterval includes two networks, and it is imperative to mitigate drastic changes in the hypernetwork output weights after learning of subsequent CL tasks while being able to gain new knowledge. The pseudocode of HyperInterval is presented in Appendix C.

Hypernetwork as a meta-trainer HyperInterval consists of interval embeddings propagated through the IBP-based hypernetwork and the target network. During the training of CL tasks, we ensure that consecutive embedding intervals have a non-empty intersections with the previous ones. A common part of these embeddings may be used as a universal embedding and applied for solving all CL tasks, see Fig. 2. Therefore, we can propagate it through the IBP-based hypernetwork, getting a single target network to classify samples from all tasks. In such a way, the hypernetwork does not have to be used in inference and thus is considered as a *meta-trainer*. Finally, one set of weights can be utilized without storing the previous ones.

In order to achieve embedding hyperrectangles overlapping for different tasks, instead of training them directly, we generated them from trained *pre-embeddings*, $a_t \in \mathbb{R}^M$, with the following formulae

$$\begin{aligned} e_t &= (\gamma/M) \cos(a_t), \\ \underline{e}_t &= e_t - \gamma \cdot \sigma(\epsilon_t), \\ \bar{e}_t &= e_t + \gamma \cdot \sigma(\epsilon_t), \end{aligned} \quad (4)$$

where γ is a perturbation hyperparameter and M is a natural number representing the embedding space dimensionality, and $\sigma(\cdot)$ is the softmax function.

At the end of the training, we have a sequence $([\underline{e}_1, \bar{e}_1], \dots, [\underline{e}_T, \bar{e}_T])$ of interval embeddings dedicated to consecutive CL tasks. The above procedure forces such segments to have non-empty intersections as it is shown in Lemma 3.1. Therefore, we can define a universal embedding as $[\underline{e}, \bar{e}] = \bigcap_t [\underline{e}_t, \bar{e}_t]$. As mentioned above, when ϵ^* is trainable, finding a universal embedding is not guaranteed.

Lemma 3.1. *Let (e_1, e_2, \dots, e_T) be embedding centers, T be the number of CL tasks, $\gamma > 0$ be a perturbation value, $\mathcal{H}(\cdot; \eta)$ be a hypernetwork with weights η , and M be a natural number representing the dimensionality of the embedding space, $\underline{e}_t, \bar{e}_t$ be calculated according to (4) with $\epsilon_t \equiv \epsilon^*$ being a vector of ones, where $t \in \{1, 2, \dots, T\}$. Then*

$$[\underline{e}, \bar{e}] = \bigcap_{t=1}^T [\underline{e}_t, \bar{e}_t]$$

has a non-empty intersection.

The proof of Lemma 3.1 is presented in Appendix E. Elements from the intersection allow one to solve multiple tasks simultaneously. Then, we can use the center of the universal embedding and the trained hypernetwork to produce a single target network. In the evaluation, it is sufficient to use such prepared target weights, and we no longer need to store the hypernetwork and trained interval embeddings.

Guarantees of non-forgetting Below, we specify the conditions of our proposed architecture to be non-forgetting. When the intersection of embedding intervals is non-empty, and the regularization for the hypernetwork training is effective, then we achieve non-forgetting, as the theorem below specifies.

Theorem 3.2. *Let (e_1, \dots, e_T) be embedding centers with corresponding perturbation vectors $(\epsilon_1, \dots, \epsilon_T)$, T be the number of CL tasks, $D_t = (X_t, Y_t)$ be a pair of observations X_t and their corresponding one-hot encoded classes Y_t taken from the t -th task, $\mathcal{H}(\cdot; \eta_T)$ be a hypernetwork with weights η_T obtained at the end of training the T -th task. Let also $\phi(\cdot; \mathcal{H}([\underline{e}_t, \bar{e}_t]; \eta_T))$ be a target network with interval weights produced by the hypernetwork such that for every $\epsilon > 0$, $t \in \{1, 2, \dots, T\}$, e_t, ϵ_t , and $x \in X_t$, there exists $y \in Y_t$ such that*

$$\sup_{\mu \in [\underline{e}_t, \bar{e}_t]} \|y - \phi(x, \mathcal{H}(\mu; \eta_T))\|_2 \leq \epsilon.$$

Assume also that $\bigcap_{t=1}^T [\underline{e}_t, \bar{e}_t]$ is non-empty and let us introduce

$$\begin{aligned} A_t &= \{\mu | \forall \epsilon > 0 \forall x \in X_t \exists y \in Y_t \\ &\quad \sup_{\mu \in [\underline{e}_t, \bar{e}_t]} \|y - \phi(x, \mathcal{H}(\mu; \eta_T))\|_2 \leq \epsilon\}, \\ &t \in \{1, 2, \dots, T\}, \end{aligned}$$

$$\begin{aligned} A &= \{\mu | \forall \epsilon > 0 \forall x \in X_t \exists y \in Y_t \\ &\quad \sup_{\mu \in \bigcap_{t=1}^T [\underline{e}_t, \bar{e}_t]} \|y - \phi(x, \mathcal{H}(\mu; \eta_T))\|_2 \leq \epsilon\}. \end{aligned}$$

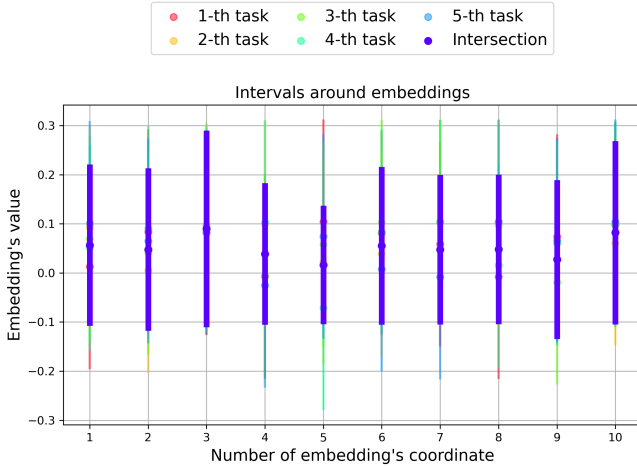


Figure 2: Embedding intervals for Split CIFAR-100, 5 tasks with 20 classes each, using the $\cos(\cdot)$ nesting method. The ten first embedding coordinates are shown.

Then, we have guarantees of non-forgetting within the region $[\underline{e}, \bar{e}] = \bigcap_{t=1}^T [\underline{e}_t, \bar{e}_t]$, i.e. $A \subset A_t$, for each $t \in \{1, 2, \dots, T\}$.

The proof of the above theorem is in Appendix E.

Entropy for Intervals Intervals can also be useful for predicting the task’s identity during an inference stage when it is unknown. In this setup, we assume that perturbation vectors are learnable parameters. Let us assume we have given some observation x from task $t_x \in \{1, 2, \dots, T\}$ whose identity is unknown. Intervals around embedding centers are propagated to interval predictions of the last layer of the target network. This implies we can utilize additional information about the probability of x . Intuitively, the selection of the t_x -th embedding should produce shorter intervals around the predictions for the x observation than the selection of embedding of other tasks. Let $\hat{p}_{x,t}$ be a vector of class probabilities produced by the target network whose weights are selected by the t -th task embedding, i.e.,

$$[\underline{z}_{x,t}, \bar{z}_{x,t}] = \phi(x; \mathcal{H}(e_t; \eta)), \quad \hat{p}_{x,t} = \sigma((z_{x,t} + \bar{z}_{x,t})/2).$$

We are going to apply this property, modifying the classical entropy as

$$H(x; t) = - \sum_{i=1}^N \frac{\hat{p}_{x,t}^{(i)} \log \hat{p}_{x,t}^{(i)}}{\bar{z}_{x,t}^{(i)} - \underline{z}_{x,t}^{(i)} + \zeta}, \quad (5)$$

where $\zeta > 0$ is a small constant added to the denominator to prevent division by zero. Finally, we choose the task’s identity simply as $\hat{t} = \arg \min_{t \in \{1, 2, \dots, T\}} H(x, t)$.

4 Experiments

In this section, we provide an overview of the results of our method under different training assumptions. We cover a variety of incremental learning setups to ensure a broad analysis of the interval arithmetic approach in CL. Moreover,

Table 1: Average accuracy with a standard deviation of different continual learning methods in the task incremental setup. Results for different methods than HyperInterval are derived from other papers.

| Method | Permuted MNIST | Split MNIST | Split CIFAR-100 | Tiny ImageNet |
|---------------|-------------------|-------------------|-------------------|-------------------|
| HAT | 97.67 0.02 | — | 72.06 0.50 | — |
| GPM | 94.96 0.07 | — | 73.18 0.52 | 67.39 0.47 |
| PackNet | 96.37 0.04 | — | 72.39 0.37 | 55.46 1.22 |
| SupSup | 96.31 0.09 | — | 75.47 0.30 | 59.60 1.05 |
| La-MaML | — | — | 71.37 0.67 | 66.99 1.65 |
| FS-DGPM | — | — | 74.33 0.31 | 70.41 1.30 |
| WSN, 30% | 96.41 0.07 | — | 75.98 0.68 | 70.92 1.37 |
| WSN, 50% | 96.24 0.11 | — | 76.38 0.34 | 69.06 0.82 |
| EWC | 95.96 0.06 | 99.12 0.11 | 72.77 0.45 | — |
| SI | 94.75 0.14 | 99.09 0.15 | — | — |
| DGR | 97.51 0.01 | 99.61 0.02 | — | — |
| HNET | 97.57 0.02 | 99.79 0.01 | — | — |
| HyperInterval | 97.78 0.09 | 99.75 0.08 | 77.46 1.34 | 66.10 0.62 |

Table 2: CL in the class incremental setup. The task identity results for universal embedding, interval entropy and vanilla entropy approaches. Vanilla entropy (VE), Interval entropy (IE), Universal Embedding (UE). Last – last task accuracy (max), Avg. – average task accuracy (max)

| Method | Permuted MNIST | Split MNIST | Split CIFAR-100 | |
|--------------------|-------------------|-------------------|-----------------|-------------|
| | | | Last | Avg. |
| HNET+ENT* | 91.75 0.21 | 69.48 0.80 | - | - |
| EWC* | 33.88 0.49 | 19.96 0.07 | - | - |
| SI* | 29.31 0.62 | 19.99 0.06 | - | - |
| DGR* | 96.38 0.03 | 91.79 0.32 | - | - |
| Euclidean-NCM** | - | - | 30.6 | 50.0 |
| FeTrIL** | - | - | 46.2 | 61.3 |
| FeCAM** | - | - | 48.1 | 62.3 |
| HyperInterval (UE) | 88.61 0.76 | 78.80 5.39 | 15.36 | 14.22 |
| HyperInterval (IE) | 94.90 0.77 | 55.37 4.24 | 48.15 | 41.03 |
| HyperInterval (VE) | 94.60 1.11 | 55.38 4.89 | 30.9 | 39.99 |

we show the best results obtained on each dataset using our training method.

Table 3: Average test accuracy with a standard deviation of the InterContiNet and HyperInterval methods, when the task identity is known or unknown, respectively. Results for InterContiNet are derived from (Wołczyk et al. 2022). The standard deviations for Split MNIST and Split CIFAR-10 are calculated over 5 seeds. The standard deviation for CIFAR-100 is calculated over 3 seeds.

| | Method | Split MNIST | Split CIFAR-10 | Split CIFAR-100 |
|-----|---------------|-------------------|-------------------|-------------------|
| TIL | InterContiNet | 98.93 0.05 | 72.64 1.18 | 42 0.2 |
| | HyperInterval | 99.75 0.08 | 90.91 0.95 | 79.23 0.36 |
| CIL | InterContiNet | 40.73 3.26 | 19.07 0.15 | — |
| | HyperInterval | 78.8 5.39 | 72.87 2.2 | — |

Training setup We apply two typical CL training setups: Task Incremental Learning (TIL), in which the task identity of test samples is known, and Class Incremental Learning (CIL), in which the task identity during inference is unknown. When we consider HyperInterval in TIL, we do not use any nesting approaches and the input embedding intervals can be of different lengths. In CIL, we use the $\cos(\cdot)$ nesting method for the embeddings and the input intervals are of the same lengths, to prevent the embeddings from collapsing to a trivial point. A more detailed description of these setups can be found in Appendix G.

Datasets We conduct experiments on 5 publicly available datasets: Permuted MNIST (von Oswald et al. 2020), Split MNIST (von Oswald et al. 2020), Split CIFAR-10 (Wołczyk et al. 2022), Split CIFAR-100 (Goswami et al. 2024) and TinyImageNet (Goswami et al. 2024). We encourage the reader to proceed to the supplementary materials for the details about the task division.

Architectures and baselines As target networks for Permuted MNIST and Split MNIST, we use two-layered MLPs with 1000 neurons per layer for the first dataset and 400 neurons per layer for the second one. For Split CIFAR-100 with 5 and 10 tasks, each with equally distributed labels per task, and for TinyImageNet, we select a convolutional network, specifically the ResNet-18, as in (Goswami et al. 2024). To ensure a fair comparison with the InterContiNet method, we also train the AlexNet architecture for Split CIFAR-10 and Split CIFAR-100 (20 tasks, each with 5 labels). We modify the AlexNet architecture according to (Wołczyk et al. 2022). Specifically, we add batch normalization after each convolutional and fully connected layer. However, we do not include batch normalization after the final linear layer, as it serves as the classification layer. Due to limited GPU resources, the number of neurons in the first two fully connected layers is reduced by half, compared to the version of AlexNet used in (Wołczyk et al. 2022). In all cases, the hypernetwork is an MLP with either one or two hidden layers. Whenever a convolutional target network is used, we apply interval relaxation during training. The description of this approach can be found in the Appendix F. We compare our solution with InterContiNet (Wołczyk et al. 2022), WSN (Kang et al. 2023), HNET (von Oswald et al. 2019), FeCAM (Goswami et al. 2024), as well as some other strong CL approaches mentioned in (Goswami et al. 2024). The choice of methods used for comparison depends on the applied training setup.

Experimental results Results for the known task identity setup are presented in Table 1. Our method outperforms its competitors on Permuted MNIST and Split CIFAR-100 datasets while reaching the second-best result on the Split MNIST dataset. Moreover, on TinyImageNet, we obtained stable results, meaning the second-lowest standard deviation score. For the same training setup, the comparison between InterContiNet and HyperInterval is shown in Table 3. We obtained better results on all three datasets used, specifically showing the advantage of HyperInterval in case of training convolutional networks. In this table, results for Split CIFAR-100 are obtained and compared using the InterCon-

tiNet setup: 20 tasks with 5 classes each.

Results for the unknown task identity setup are presented in Tables 2 and 3. Despite the large standard deviation on Split MNIST, we obtain one universal embedding which solves all tasks at once, as we do for Permuted MNIST. On Split CIFAR-100 we obtain the best maximum last task accuracy. Moreover, compared to other methods, HyperInterval achieves a smaller deviation between the last task and average task accuracy, showing consistency in consecutive task results. Unfortunately, the universal embedding found by HyperInterval performs poorly on the Split CIFAR-100 dataset, achieving only approximately 15% accuracy. We argue that this is due to the larger number of classes per task, which makes it challenging to identify a single universal embedding capable of solving such tasks simultaneously. As in the previous setup, HyperInterval method outperforms InterContiNet on all datasets by a large margin, which is shown in Table 3. In Figure 2 we present the interval embeddings for each of 5 tasks of Split CIFAR-100. It is shown that a non-empty universal embedding exists, moreover, it does not collapse to a point in the embedding space.

In Appendix H we present a study focused on interval lengths, interval nesting and regularization. In Appendix I we present more detailed insight of the above experimental results.

5 Conclusions and limitations

In this paper, we introduce HyperInterval, a continual learning architecture that employs interval arithmetic in the trained neural model and a hypernetwork producing its weights. HyperInterval uses interval embeddings for consecutive tasks and trains the hypernetwork to transform these embeddings into weights of the target network. The proposed mechanism allows us to train interval networks on large datasets in continual learning scenarios, in the task incremental- and class incremental setups. HyperInterval enables the generation of a universal embedding thanks to interval arithmetic and hypernetwork training. The intersection of intervals, i.e. a universal embedding, can solve all tasks simultaneously. In such a scenario, the hypernetwork functions solely as a *meta-trainer*, meaning that we maintain only a single set of weights generated by the hypernetwork through the universal embedding. This approach significantly reduces memory usage. Furthermore, we provide formal guarantees of non-forgetting.

Limitations Non-forgetting guarantees within the interval parameter space generated by the hypernetwork are valid only as long as the hypernetwork’s regularization term remains effective. Second, we have observed that achieving satisfactory performance becomes challenging when the number of classes in a given task is large. Splitting such a task into subtasks may be advantageous and subsequently finding a universal embedding, but we leave this for future work.

A Interval arithmetic in neural networks

Suppose $A, B \subset \mathbb{R}$ represent intervals. For all $\bar{a}, \underline{a}, \bar{b}, \underline{b} \in \mathbb{R}$, where $A = [\underline{a}, \bar{a}]$ and $B = [\underline{b}, \bar{b}]$, arithmetic operations can

be defined as in (Lee 2004):

- addition: $[a, \bar{a}] + [b, \bar{b}] = [a + b, \bar{a} + \bar{b}]$
- multiplication: $[a, \bar{a}] * [b, \bar{b}] = [\min(a * \underline{b}, \underline{a} * \bar{b}, \bar{a} * \underline{b}, \underline{a} * \bar{b}), \max(\underline{a} * \underline{b}, \underline{a} * \bar{b}, \bar{a} * \underline{b}, \bar{a} * \bar{b})]$

Therefore, interval arithmetic is capable of executing affine transformations, enabling the implementation of both fully-connected and convolutional layers in neural networks.

We denote by $\phi(x; \theta)$ a layered neural classifier with input x and weights θ . It comprises a series of transformations

$$\phi(x; \theta) = (h_L \circ h_{L-1} \circ \dots \circ h_1)(x; \theta) \quad (6)$$

$$= h_L(h_{L-1}(\dots h_1(x))). \quad (7)$$

All component transformations, h_l , are also based on the weights θ , which we omit in the notation. The final output $\phi(x; \theta) = z_L \in \mathbb{R}^N$ is to indicate one of N classes to which the input x belongs.

In InterContiNet (Wołczyk et al. 2022), weight matrices and bias vectors of each layer h_l are located in hyperrectangles $[W_l, \bar{W}_l]$ and $[b_l, \bar{b}_l]$, respectively. We denote $[\theta, \bar{\theta}] = \langle [W_1, \bar{W}_1], [b_1, \bar{b}_1], \dots, [W_L, \bar{W}_L], [b_L, \bar{b}_L] \rangle$ to represent intervals of all the trainable parameters in the network.

The transformation in l -th layer, $l = 1, \dots, L$, of InterContiNet can be expressed as:

$$[z_l, \bar{z}_l] = h_l([z_{l-1}, \bar{z}_{l-1}]) \quad (8)$$

where $z_0 = [x, x]$ is the input, $[z_l, \bar{z}_l]$ is the hyperrectangle of l -th layer activations,

$$h_l([z_{l-1}, \bar{z}_{l-1}]) = [h_l, \bar{h}_l]([z_{l-1}, \bar{z}_{l-1}]) \quad (9)$$

$$= \psi([W_l, \bar{W}_l][z_{l-1}, \bar{z}_{l-1}] + [b_l, \bar{b}_l]), \quad (10)$$

with ψ being an activation function with positive output, and

$$z_l = \min_{z_{l-1} \leq z_{l-1} \leq \bar{z}_{l-1}} h_l(z_{l-1}), \quad (11)$$

$$\bar{z}_l = \max_{z_{l-1} \leq z_{l-1} \leq \bar{z}_{l-1}} h_l(z_{l-1}). \quad (12)$$

Monotonicity of ψ (e.g., ReLU, logistic sigmoid) is enough for efficient computation of $[z_l, \bar{z}_l]$.

The input $z_0 = [x, x]$ is assumed to be nonnegative, $x \geq 0$. The final output $\phi(z_0; [\theta_1, \bar{\theta}_L]) = h_L(h_{L-1}(\dots h_1(z_0))) = [z_L, \bar{z}_L]$ comprises N intervals, one for each class.

B Layered hypernetwork with interval embedding input

Let the hypernetwork $\mathcal{H}([e_t, \bar{e}_t]; \eta)$ comprise a series of transformations $[h_1, \bar{h}_1](\cdot), \dots, [h_L, \bar{h}_L](\cdot)$ across its L layers. The final output $[h_L, \bar{h}_L]([h_{L-1}, \bar{h}_{L-1}]([\dots [h_1, \bar{h}_1]([x, x])])) = [z_L, \bar{z}_L]$ produces interval weights for the target model. This result represents a composition of weight intervals of consecutive layers.

In HyperInterval, we propagate the interval embedding $[z_0, \bar{z}_0] = [e, \bar{e}]$ from the input to the output layer. The output

bounding box $[z_l, \bar{z}_l]$ from the hypernetwork $\mathcal{H}([e_t, \bar{e}_t]; \eta)$ is calculated in the following way:

$$\mu_{l-1} = \frac{\bar{z}_{l-1} + z_{l-1}}{2}, \quad r_{l-1} = \frac{\bar{z}_{l-1} - z_{l-1}}{2},$$

$$\mu_l = W_l \mu_{l-1} + b_l, \quad r_l = |W_l| r_{l-1},$$

$$z_l = \psi(\mu_l - r_l), \quad \bar{z}_l = \psi(\mu_l + r_l),$$

where W_l and b_l are l -th layer weight matrix and bias vector, respectively, $\eta = \langle W_1, b_1, W_2, b_2, \dots, W_L, b_L \rangle$, and $|\cdot|$ is an element-wise absolute value operator.

Therefore, our interval hypernetwork $\mathcal{H}([e_t, \bar{e}_t]; \eta) = [\theta_t, \bar{\theta}_t]$ transforms the embedding of the t -th task into interval weights of the target network.

HyperInterval In HyperInterval, trainable interval embeddings $[e_t, \bar{e}_t]$ are used for producing separated network weights for each continuous learning task $t, t \in \{1, \dots, T\}$. These embeddings are propagated through the trainable IBP-based hypernetwork

$$\mathcal{H}([e_t, \bar{e}_t]; \eta) = [\theta_t, \bar{\theta}_t]$$

into interval weights of the target model. To derive the equations for linear layers, we introduce the following terms:

$$W_{k-1}^+ = \max\{W_{k-1}, 0\}, \quad W_{k-1}^- = \max\{-W_{k-1}, 0\},$$

$$\bar{W}_{k-1}^+ = \max\{\bar{W}_{k-1}, 0\}, \quad \bar{W}_{k-1}^- = \max\{-\bar{W}_{k-1}, 0\},$$

where $k \in \{2, \dots, L\}$, $[\theta_t, \bar{\theta}_t] = \langle [W_1, \bar{W}_1], [b_1, \bar{b}_1], \dots, [W_L, \bar{W}_L], [b_L, \bar{b}_L] \rangle$, $\min\{\cdot, \cdot\}$ and $\max\{\cdot, \cdot\}$ denote element-wise minimum and maximum operations. Then, one need to calculate such an expression:

$$[z_k, \bar{z}_k] = \psi([W_{k-1}, \bar{W}_{k-1}] \cdot [z_{k-1}, \bar{z}_{k-1}] + [b_{k-1}, \bar{b}_{k-1}]).$$

Based on the definition of multiplying two intervals, we obtain that:

$$\begin{aligned} & [W_{k-1}, \bar{W}_{k-1}] \cdot [z_{k-1}, \bar{z}_{k-1}] \\ &= [W_{k-1}^+ - W_{k-1}^-, \bar{W}_{k-1}^+ - \bar{W}_{k-1}^-] \cdot [z_{k-1}, \bar{z}_{k-1}] \\ &= ([W_{k-1}^+, \bar{W}_{k-1}^+] - [\bar{W}_{k-1}^-, W_{k-1}^-]) \cdot [z_{k-1}, \bar{z}_{k-1}] \\ &= [W_{k-1}^+, \bar{W}_{k-1}^+] \cdot [z_{k-1}, \bar{z}_{k-1}] \\ &\quad - [\bar{W}_{k-1}^-, W_{k-1}^-] \cdot [z_{k-1}, \bar{z}_{k-1}]. \end{aligned}$$

Generally, distributivity does not hold for interval arithmetic, which means that $([a, b] + [c, d]) \cdot [e, f]$ does not equal $[a + c, b + d] \cdot [e, f]$ for some $a, b, c, d, e, f \in \mathbb{R}$ in general. However, this property holds when the multiplication of intervals $[a, b] \cdot [c, d]$ results in an interval with non-negative endpoints. This is why the decomposition of lower and upper matrices into the subtraction of positive and negative matrices is useful. Using the definition of interval multiplication and the fact that $W_{k-1}^+, \bar{W}_{k-1}^+, W_{k-1}^-, \bar{W}_{k-1}^-, z_{k-1}, \bar{z}_{k-1} \geq 0$, we have:

$$\begin{aligned} & [W_{k-1}^+, \bar{W}_{k-1}^+] \cdot [z_{k-1}, \bar{z}_{k-1}] \\ &= \left[\begin{array}{cc} \min_{a \in \{W_{k-1}^+, \bar{W}_{k-1}^+\}} \{a \cdot b\}, & \max_{a \in \{W_{k-1}^+, \bar{W}_{k-1}^+\}} \{a \cdot b\} \\ b \in \{z_{k-1}, \bar{z}_{k-1}\} & b \in \{z_{k-1}, \bar{z}_{k-1}\} \end{array} \right] \\ &= [W_{k-1}^+ \cdot z_{k-1}, \bar{W}_{k-1}^+ \cdot \bar{z}_{k-1}]. \end{aligned}$$

Analogously,

$$\begin{aligned} & [\bar{W}_{k-1}^-, W_{k-1}^-] \cdot [\underline{z}_{k-1}, \bar{z}_{k-1}] \\ &= \left[\begin{array}{cc} \min_{\substack{a \in \{W_{k-1}^+, \bar{W}_{k-1}^+\} \\ b \in \{\underline{z}_{k-1}, \bar{z}_{k-1}\}}} \{a \cdot b\}, & \max_{\substack{a \in \{W_{k-1}^-, \bar{W}_{k-1}^-\} \\ b \in \{\underline{z}_{k-1}, \bar{z}_{k-1}\}}} \{a \cdot b\} \end{array} \right] \\ &= [\bar{W}_{k-1}^- \cdot \underline{z}_{k-1}, W_{k-1}^- \cdot \bar{z}_{k-1}] \\ &= -[-W_{k-1}^- \cdot \bar{z}_{k-1}, -\bar{W}_{k-1}^- \cdot \underline{z}_{k-1}], \end{aligned}$$

which gives us the final form of the equations:

$$\begin{aligned} \underline{z}_k &= \psi(W_{k-1}^+ \cdot \underline{z}_{k-1} - W_{k-1}^- \cdot \bar{z}_{k-1} + \underline{b}_{k-1}), \\ \bar{z}_k &= \psi(\bar{W}_{k-1}^+ \cdot \bar{z}_{k-1} - \bar{W}_{k-1}^- \cdot \underline{z}_{k-1} + \bar{b}_{k-1}). \end{aligned}$$

Since the equations above are derived for propagation through fully connected layers, a similar version for convolutional layers can be easily obtained, as a convolution operation can be expressed as a multiplication operation. The final form of these equations is as follows:

$$\begin{aligned} \underline{z}_k &= \psi(W_{k-1}^+ * \underline{z}_{k-1} - W_{k-1}^- * \bar{z}_{k-1} + \underline{b}_{k-1}), \\ \bar{z}_k &= \psi(\bar{W}_{k-1}^+ * \bar{z}_{k-1} - \bar{W}_{k-1}^- * \underline{z}_{k-1} + \bar{b}_{k-1}), \end{aligned}$$

where the $*$ operator denotes the convolution operation. Unfortunately, such equations cannot be easily obtained for batch normalization layers.

C The HyperInterval algorithm

HyperInterval is presented below as Algorithm 1.

D Lipschitz regularity of an interval-based hypernetwork

Proposition 1. *Let (e_1, e_2, \dots, e_T) be embedding centers, T be the number of CL tasks, $\gamma > 0$ be a perturbation value, $\mathcal{H}(\cdot; \eta)$ be an MLP-based hypernetwork with weights $\eta = \langle \eta_1, b_1, \dots, \eta_L, b_L \rangle$ and an activation function, $\psi(\cdot)$, is Lipschitz continuous with a real positive constant K , M be a natural number representing the dimensionality of the embedding space, e_t, \bar{e}_t be calculated according to Section 3.2 (4) with $\epsilon_t \equiv \epsilon^*$ being a vector of ones, where $t \in \{1, 2, \dots, T\}$, L be a number of the hypernetwork's layers. Then, for each t*

$$\sup_{\mu, \xi \in [e_t, \bar{e}_t]} \|\mathcal{H}(\mu; \eta) - \mathcal{H}(\xi; \eta)\|_2 \leq K^L \prod_{i=1}^L \|\eta_i\|_2 \|e_t - \bar{e}_t\|_2.$$

Proof of Proposition 1. From Proposition 1, (Virmaux and Scaman 2018), and the fact that the hypernetwork is an MLP-based neural network with a Lipschitz continuous activation function, for any $\mu, \xi \in [e_t, \bar{e}_t]$, $t \in \{1, \dots, T\}$, we have:

$$\|\mathcal{H}(\mu; \eta) - \mathcal{H}(\xi; \eta)\|_2 \leq K^L \prod_{i=1}^L \|\eta_i\|_2 \cdot \|\mu - \xi\|_2.$$

It now suffices to take the supremum over $\mu, \xi \in [e_t, \bar{e}_t]$ on both sides of the above inequality:

$$\sup_{\mu, \xi \in [e_t, \bar{e}_t]} \|\mathcal{H}(\mu; \eta) - \mathcal{H}(\xi; \eta)\|_2 \leq K^L \prod_{i=1}^L \|\eta_i\|_2 \|e_t - \bar{e}_t\|_2,$$

Algorithm 1: The pseudocode of HyperInterval.

Require: hypernetwork \mathcal{H} with weights η , target network ϕ , softmax function $\sigma(\cdot)$, perturbation value $\gamma > 0$, regularization strength $\beta > 0$, cross-entropy components strength $\kappa \in (0, 1)$, dimensionality of the embedding space M , n training iterations, datasets $\{D_1, D_2, \dots, D_T\}$, $(x_{i,t}, y_{i,t}) \in D_t, t \in \{1, \dots, T\}$, $i \in \{1, \dots, N_t\}$, N_t is a number of samples in the dataset D_t .

Ensure: updated hypernetwork \mathcal{H} weights η

Initialize randomly weights η with pre-embeddings (a_1, a_2, \dots, a_T) and corresponding perturbation vectors $(\epsilon_1^*, \epsilon_2^*, \dots, \epsilon_T^*)$

for $t \leftarrow 1$ to T **do**

if $t > 1$ **then**

$\eta^* \leftarrow \eta$

for $t' \leftarrow 1$ to $t - 1$ **do**

$\epsilon_{t'}^* \leftarrow \gamma \cdot \sigma(\epsilon_{t'}^*)$

Store $[\theta_{t'}^*, \bar{\theta}_{t'}^*] \leftarrow$

$\leftarrow \mathcal{H}([\frac{\gamma}{M} \cos(a_{t'}) - \epsilon_{t'}^*, \frac{\gamma}{M} \cos(a_{t'}) + \epsilon_{t'}^*]; \eta^*)$

end for

end if

for $i \leftarrow 1$ to n **do**

if $i \leq \lfloor \frac{n}{2} \rfloor$ **then**

$\hat{\epsilon}_i^* \leftarrow \frac{i}{\lfloor \frac{n}{2} \rfloor} \cdot \gamma$

else

$\hat{\epsilon}_i^* \leftarrow \gamma$

end if

$\epsilon_t^* \leftarrow \hat{\epsilon}_i^* \cdot \sigma(\epsilon_t^*)$

$[\theta_t^*, \bar{\theta}_t^*] \leftarrow$

$\leftarrow \mathcal{H}([\frac{\gamma}{M} \cos(a_t) - \epsilon_t^*, \frac{\gamma}{M} \cos(a_t) + \epsilon_t^*]; \eta)$

$[\hat{y}_{i,t}, \bar{y}_{i,t}] \leftarrow \phi(x_{i,t}; [\theta_t^*, \bar{\theta}_t^*])$

if $t = 1$ **then**

$\mathcal{L} \leftarrow \mathcal{L}_{current}$

else

$\mathcal{L} \leftarrow \mathcal{L}_{current} + \beta \cdot \mathcal{L}_{output}$

end if

Update η, a_t and ϵ_t

end for

Freeze and store a_t and ϵ_t

end for

where

$$\sup_{\mu, \xi \in [e_t, \bar{e}_t]} \|\mu - \xi\|_2 = \|e_t - \bar{e}_t\|_2.$$

□

A similar result can be proven for convolutional neural networks. For more details, please see (Virmaux and Scaman 2018).

E Proof of non-forgetting in HyperInterval

Proof of Lemma 3.1. Take arbitrary $t_1, t_2 \in \{1, 2, \dots, T\}$ and i -th coordinate of the embeddings e_{t_1}, e_{t_2} , where $i \in$

$\{1, 2, \dots, M\}$. Suppose the worst-case scenario, where

$$\begin{aligned}\cos\left(e_{t_1}^{(i)}\right) &= 1, \\ \cos\left(e_{t_2}^{(i)}\right) &= -1.\end{aligned}$$

Then the absolute difference between $\frac{\gamma}{M} \cos\left(e_{t_1}^{(i)}\right)$ and $\frac{\gamma}{M} \cos\left(e_{t_2}^{(i)}\right)$ will be the biggest and can be calculated as

$$\begin{aligned}\left|\frac{\gamma}{M} \cos\left(e_{t_1}^{(i)}\right) - \frac{\gamma}{M} \cos\left(e_{t_2}^{(i)}\right)\right| &= \frac{2\gamma}{M} \\ &= 2\gamma \cdot \sigma\left(\epsilon^*\right)^{(i)}.\end{aligned}$$

Note that the maximum distance at the i -th coordinate between transformed centers of the intervals is equal to $\frac{2\gamma}{M}$, but this value is the same as $2\gamma \cdot \sigma\left(\epsilon^*\right)^{(i)}$. This means that in the worst case the intersection is a single point. As t_1, t_2 and i were chosen arbitrary, the intersection

$$[\underline{e}, \bar{e}] = \bigcap_{t=1}^T [\underline{e}_t, \bar{e}_t]$$

is non-empty, what ends the proof. \square

Proof of Theorem 3.2. As we know that the intersection $[\underline{e}, \bar{e}]$ is non-empty, we just need to show that $A_t \subset A$ for every $t \in \{1, \dots, T\}$. Please note that $\{A_t\}_{t=1}^T$ is a sequence of non-empty, compact subsets of R^N . Every compact set is bounded, it implies that

$$\sup\left(\bigcap_{t=1}^T A_t\right) = \min_{t \in \{1, \dots, T\}} \sup(A_t).$$

We can use this identity to prove that $A \subset A_{t^*}$, where $t^* \in \{1, \dots, T\}$ is arbitrary chosen. It is straightforward to see that

$$\begin{aligned}A &= \{\mu | \forall \epsilon > 0 \forall x \in X_t \exists y \in Y_t \sup_{\mu \in \bigcap_{t=1}^T [\underline{e}_t, \bar{e}_t]} C(\mu) \leq \epsilon\} \\ &= \{\mu | \forall \epsilon > 0 \forall x \in X_t \exists y \in Y_t \min_{t \in \{1, \dots, T\}} \sup_{\mu \in [\underline{e}_t, \bar{e}_t]} C(\mu) \leq \epsilon\} \\ &= \{\mu | \forall \epsilon > 0 \forall x \in X_t \exists y \in Y_t \forall t \in \{1, \dots, T\} \sup_{\mu \in [\underline{e}_t, \bar{e}_t]} C(\mu) \leq \epsilon\} \\ &= \bigcap_{t=1}^T \{\mu | \forall \epsilon > 0 \forall x \in X_t \exists y \in Y_t \sup_{\mu \in [\underline{e}_t, \bar{e}_t]} C(\mu) \leq \epsilon\} \\ &\subset \{\{\mu | \forall x \in X_t \exists y \in Y_t \sup_{\mu \in [\underline{e}_{t^*}, \bar{e}_{t^*}]} C(\mu) \leq \epsilon\}\} \\ &= A_{t^*},\end{aligned}$$

where

$$C(\mu) = \|y - \phi(x, \mathcal{H}(\mu; \eta_T))\|_2.$$

As t^* was arbitrary chosen, for each $t \in \{1, \dots, T\}$ $A \subset A_t$, what ends the proof. \square

F Relaxation technique

Based on our experiments and those conducted in (Wołczyk et al. 2022), we have observed that training convolutional neural networks in an interval-based setup presents significant challenges. We argue that many of these difficulties stem from the absence of a straightforward substitute for an interval-based batch normalization layer. To address these issues, we propose mitigating the challenges by relaxing the interval constraints in the target network while maintaining a fully interval-based hypernetwork. The pseudocode for this approach is provided in Algorithm 2.

While the relaxation technique facilitates effective training of convolutional neural networks, it also has a certain drawback - it limits applicability of the interval entropy method. This limitation arises because the image of the target network obtained through the relaxation technique is only contained within the image of the target network trained using the fully interval-based method. This outcome is illustrated in Proposition 2.

Proposition 2. *Let (e_1, e_2, \dots, e_T) be embedding centers, T be the number of CL tasks, $\gamma > 0$ be a perturbation value, $\mathcal{H}(\cdot; \eta)$ be a hypernetwork with weights η , M be a natural number representing the dimensionality of the embedding space, $\underline{e}_t, \bar{e}_t$ be calculated according to 3.2 (4) with $\epsilon_t \equiv \epsilon^*$ being a vector of ones, where $t \in \{1, 2, \dots, T\}$. Let also $\phi(\cdot; [\underline{\theta}_t, \bar{\theta}_t])$ be a target network with a non-negative and non-decreasing activation function $\psi(\cdot)$ and with interval weights generated by the hypernetwork. Then, for each $t \in \{1, \dots, T\}$ and non-negative observation x :*

$$[\phi_{\min}(x), \phi_{\max}(x)] \subseteq \phi(x; [\underline{\theta}_t, \bar{\theta}_t]),$$

where

$$\begin{aligned}\phi_{\min}(x) &= \min\{\phi(x; \underline{\theta}_t), \phi(x; \bar{\theta}_t)\}, \\ \phi_{\max}(x) &= \max\{\phi(x; \underline{\theta}_t), \phi(x; \bar{\theta}_t)\}.\end{aligned}$$

Proof. It is straightforward to see that:

$$\begin{aligned}\phi_{\min}(x) &\geq \min_{\theta \in [\underline{\theta}_t, \bar{\theta}_t]} \phi(x; \theta), \\ \phi_{\max}(x) &\leq \max_{\theta \in [\underline{\theta}_t, \bar{\theta}_t]} \phi(x; \theta).\end{aligned}$$

This ends the proof, because

$$\left[\min_{\theta \in [\underline{\theta}_t, \bar{\theta}_t]} \phi(x; \theta), \max_{\theta \in [\underline{\theta}_t, \bar{\theta}_t]} \phi(x; \theta) \right] = \phi(x; [\underline{\theta}_t, \bar{\theta}_t]).$$

\square

One might ask whether equality can occur in Proposition 2. The answer is yes, and this is demonstrated in Proposition 3.

Proposition 3. *Let us assume that all the assumptions of Proposition 2 are satisfied and that the notation is preserved. Additionally, assume that the interval weights $[\underline{\theta}_t, \bar{\theta}_t] = \langle [W_1^{(t)}, \bar{W}_1^{(t)}], [b_1^{(t)}, \bar{b}_1^{(t)}], \dots, [W_L^{(t)}, \bar{W}_L^{(t)}], [b_L^{(t)}, \bar{b}_L^{(t)}] \rangle$ produced by the hypernetwork are non-negative, where L denotes the number of layers in the target network. Then, for each $t \in \{1, \dots, T\}$ and non-negative observation x :*

$$[\phi_{\min}(x), \phi_{\max}(x)] = \phi(x; [\underline{\theta}_t, \bar{\theta}_t]).$$

Proof. Fix arbitrary $t \in \{1, \dots, T\}$ and let us introduce the following notation for any $k \in \{1, \dots, L-1\}$:

$$\begin{aligned}\bar{z}_k^{(t)} &= \psi \left(\bar{W}_k^{(t)} \cdot \bar{z}_{k-1}^{(t)} + \bar{b}_k^{(t)} \right), \\ \underline{z}_k^{(t)} &= \psi \left(W_k^{(t)} \cdot \underline{z}_{k-1}^{(t)} + \underline{b}_k^{(t)} \right), \\ \underline{z}_0^{(t)} &= x, \\ \bar{z}_0^{(t)} &= x.\end{aligned}$$

Based on the assumptions, we know that the weights generated by the hypernetwork are non-negative and that $\psi(\cdot)$ is a non-negative valued and non-decreasing activation function. This implies that for any $\underline{\alpha}_k^{(t)}, \bar{\alpha}_k^{(t)} \in [W_k^{(t)}, \bar{W}_k^{(t)}]$, $\underline{\beta}_k^{(t)}, \bar{\beta}_k^{(t)} \in [\underline{b}_k^{(t)}, \bar{b}_k^{(t)}]$ such that $\underline{\alpha}_k^{(t)} \leq \bar{\alpha}_k^{(t)}$, $\underline{\beta}_k^{(t)} \leq \bar{\beta}_k^{(t)}$, $k \in 1, \dots, L$:

$$\begin{aligned}\underline{\alpha}_k^{(t)} \cdot \underline{z}_{k-1}^{(t)} + \underline{\beta}_k^{(t)} &\leq \bar{\alpha}_k^{(t)} \cdot \bar{z}_{k-1}^{(t)} + \bar{\beta}_k^{(t)}, \\ \psi \left(\underline{\alpha}_k^{(t)} \cdot \underline{z}_{k-1}^{(t)} + \underline{\beta}_k^{(t)} \right) &\leq \psi \left(\bar{\alpha}_k^{(t)} \cdot \bar{z}_{k-1}^{(t)} + \bar{\beta}_k^{(t)} \right).\end{aligned}$$

Hence,

$$\begin{aligned}W_L^{(t)} \cdot \underline{z}_{L-1}^{(t)} + \underline{b}_L^{(t)} &= \phi_{\min}(x), \\ W_k^{(t)} \cdot \underline{z}_{k-1}^{(t)} + \underline{b}_k^{(t)} &= \min_{\substack{a \in \{W_k^{(t)}, \bar{W}_k^{(t)}\} \\ b \in \{\underline{z}_{k-1}^{(t)}, \bar{z}_{k-1}^{(t)}\}}} \{a \cdot b + \underline{b}_k^{(t)}\}.\end{aligned}$$

Analogously,

$$\begin{aligned}\bar{W}_L^{(t)} \cdot \bar{z}_{L-1}^{(t)} + \bar{b}_L^{(t)} &= \phi_{\max}(x), \\ \bar{W}_k^{(t)} \cdot \bar{z}_{k-1}^{(t)} + \bar{b}_k^{(t)} &= \max_{\substack{a \in \{W_k^{(t)}, \bar{W}_k^{(t)}\} \\ b \in \{\underline{z}_{k-1}^{(t)}, \bar{z}_{k-1}^{(t)}\}}} \{a \cdot b + \bar{b}_k^{(t)}\}.\end{aligned}$$

Then,

$$\begin{aligned}[\phi_{\min}(x), \phi_{\max}(x)] &= \left[W_L^{(t)}, \bar{W}_L^{(t)} \right] \cdot \left[\underline{z}_{L-1}^{(t)}, \bar{z}_{L-1}^{(t)} \right] \\ &\quad + \left[\underline{b}_L^{(t)}, \bar{b}_L^{(t)} \right] \\ &= \phi(x, [\underline{\theta}_t, \bar{\theta}_t]),\end{aligned}$$

what ends the proof. \square

G Training details

Datasets and CL setup We use the following datasets: 1) Permuted MNIST-10 (von Oswald et al. 2020), consisting of 28x28 pixel grey-scale images of 10 classes of digits, where each task is obtained by applying a random permutation to the input image pixels, with a typical length of $T = 10$ tasks; 2) Split MNIST (von Oswald et al. 2020), containing tasks designed by sequentially pairing the digits to introduce task overlap, forming $T = 5$ binary classification tasks; 3) Split CIFAR-100 (Goswami et al. 2024), consisting of 32x32 pixel color images of 100 classes; 4) Split CIFAR-10 (Wołczyk et al. 2022), with $T = 5$ binary classification tasks; 5) TinyImageNet (Goswami et al. 2024), a subset of

Algorithm 2: The pseudocode of HyperInterval relaxation technique.

Require: hypernetwork \mathcal{H} with weights η , target network ϕ , softmax function $\sigma(\cdot)$, perturbation value $\gamma > 0$, regularization strength $\beta > 0$, cross-entropy components strength $\kappa \in (0, 1)$, dimensionality of the embedding space M , n training iterations, datasets $\{D_1, D_2, \dots, D_T\}$, $(x_{i,t}, y_{i,t}) \in D_t, t \in \{1, \dots, T\}$, $i \in \{1, \dots, N_t\}$, N_t is a number of samples in the dataset D_t .

Ensure: updated hypernetwork \mathcal{H} weights η
Initialize randomly weights η with pre-embeddings (a_1, a_2, \dots, a_T) and corresponding perturbation vectors $(\epsilon_1^*, \epsilon_2^*, \dots, \epsilon_T^*)$

for $t \leftarrow 1$ to T **do**

if $t > 1$ **then**

$\eta^* \leftarrow \eta$

for $t' \leftarrow 1$ to $t-1$ **do**

$\epsilon_{t'}^* \leftarrow \gamma \cdot \sigma(\epsilon_{t'}^*)$

Store $[\theta_{t'}^*, \bar{\theta}_{t'}^*] \leftarrow$

$\leftarrow \mathcal{H}(\left[\frac{\gamma}{M} \cos(a_{t'}) - \epsilon_{t'}^*, \frac{\gamma}{M} \cos(a_{t'}) + \epsilon_{t'}^*\right]; \eta^*)$

end for

end if

for $i \leftarrow 1$ to n **do**

if $i \leq \lfloor \frac{n}{2} \rfloor$ **then**

$\hat{\epsilon}_i^* \leftarrow \left[\frac{i}{\frac{n}{2}} \right] \cdot \gamma$

else

$\hat{\epsilon}_i^* \leftarrow \gamma$

end if

$\epsilon_t^* \leftarrow \hat{\epsilon}_i^* \cdot \sigma(\epsilon_t^*)$

$[\theta_t, \bar{\theta}_t] \leftarrow$

$\leftarrow \mathcal{H}(\left[\frac{\gamma}{M} \cos(a_t) - \epsilon_t^*, \frac{\gamma}{M} \cos(a_t) + \epsilon_t^*\right]; \eta)$

$\hat{y}_{i,t} \leftarrow \phi(\mathbf{x}_{i,t}; \theta_t)$

$\bar{y}_{i,t} \leftarrow \phi(\mathbf{x}_{i,t}; \bar{\theta}_t)$

$\left[\hat{y}_{i,t}, \bar{y}_{i,t} \right] \leftarrow \left[\min\{\hat{y}_{i,t}, \bar{y}_{i,t}\}, \max\{\hat{y}_{i,t}, \bar{y}_{i,t}\} \right]$

if $t = 1$ **then**

$\mathcal{L} \leftarrow \mathcal{L}_{\text{current}}$

else

$\mathcal{L} \leftarrow \mathcal{L}_{\text{current}} + \beta \cdot \mathcal{L}_{\text{output}}$

end if

Update η , a_t and ϵ_t

end for

Freeze and store a_t and ϵ_t

end for

ImageNet (Russakovsky et al. 2015), consisting of 64x64 pixel color images of 200 classes; 6) Permuted MNIST-100 (Goswami et al. 2024), similar to the Permuted MNIST-10 dataset, but with $T = 100$ tasks, 10 classes each, only used in the ablation study. When the task identity is unknown during inference, for Split CIFAR-100 we experiment with a setup of 5 tasks with 20 classes each, we do not conduct experiments on TinyImageNet in this setup. When the task identity is known, we pick a setup with 10 tasks with 10 classes each and 20 tasks with 5 classes each for Split CIFAR-100 and 40

tasks with 5 classes each for TinyImageNet.

Training setups We consider two training setups. When the task identity is known in the test phase, during training the perturbation value γ is multiplied by a learnable vector and thus intervals are a learned parameter, which might result in them being of different lengths. When the task identity is unknown during the inference time, the perturbation value γ is multiplied by a fixed value normalized vector and consequently intervals are of equal length. The latter setup is to prevent the nested intervals from having empty intersection in the embedding space.

Relaxation technique Depending on the complexity of the target network architecture, we have two interval learning approaches: 1) fully interval technique, meaning that we apply intervals to both the hypernetwork and target network; 2) interval relaxation technique, meaning we use a fully interval hypernetwork and a non-interval target network, where we only restore the order of predictions after its last layer, hence we can also use vanilla batch normalization. Regardless of the training setup (known / unknown task identity): 1) for target networks which are MLPs, we always use the fully interval training technique; 2) in cases when a convolutional target network is used (ResNet-18 and AlexNet), we apply the interval relaxation technique to the training process, since convolutional layers are generally more difficult to train with intervals (Wolczyk et al. 2022).

Form of hypernetwork regularization loss The interval weights produced by the hypernetwork are contained within the interval

$$\left[\min_{\mu \in [\underline{e}_t, \bar{e}_t]} \mathcal{H}(\mu; \eta), \max_{\mu \in [\underline{e}_t, \bar{e}_t]} \mathcal{H}(\mu; \eta) \right].$$

As previously mentioned, the interval weights produced by the hypernetwork tend to be short, and regularization of the interval endpoints is typically sufficient. However, it is worth considering what would happen if regularization were applied to points within the interval that are not endpoints. We examined three types of regularization: (1) regularization applied only to the endpoints of the interval, (2) regularization applied to both the endpoints and the midpoint of the interval, and (3) regularization applied to the endpoints and randomly selected points from within the interval. We observed that the second and third approaches yielded slightly better results than the first. Although there was no significant difference between the second and third approaches, we opted to use the second approach.

Common hyperparameters In each training process, we use the ReLU activation function and apply the Adam optimizer with different learning rates but the same default betas coefficients, i.e., $\beta_1 = 0.9$, $\beta_2 = 0.999$. Also, anytime we specify that a learning rate scheduler is used, we apply the ReduceLROnPlateau scheduler from PyTorch. There is a parameter κ which is responsible for weighing the worst case loss wrt. to the basic entropy loss, as it takes part in their convex linear combination. We always use $\kappa = 0.5$. However, this hyperparameter is scheduled during training, so instead of using the same κ value throughout the training, we use

$\kappa_i = \max\{1 - 0.00005 \cdot i, \kappa\}$, where i is the current training iteration. In other words, it means that at the beginning of the training we put more attention to the proper classification on the centers of the intervals and then, gradually, we put more attention to the worst case component. Furthermore, there is another parameter, namely β , which is responsible for the hypernetwork regularization strength, weighing the part of loss responsible for non-forgetting.

Hardware and software resources used We implemented HyperInterval using Python 3.7.6, incorporating libraries such as hypnettorch 0.0.4 (von Oswald et al., 2019), PyTorch 1.5.0 with CUDA support, NumPy 1.18, Pandas 1.0.1, Matplotlib 3.1.3, seaborn 0.10.0, among others. Most of our computations are conducted on an NVIDIA GeForce RTX 4090, but some training sessions are also performed using NVIDIA GeForce RTX 3080, NVIDIA GeForce RTX 2070, NVIDIA A100, and NVIDIA DGX graphic cards.

Known task identity hyperparameters As it was stated in the main section of this work, here we do not use any interval nesting methods. Also, in this setting, we randomly initialize each task embedding. Let us cover the list of parameters used in this setup:

- Split MNIST – the hypernetwork and target network used are two-layered MLPs with 75 neurons per layer and 400 neurons per layer, respectively. We use data augmentation as in (von Oswald et al. 2019), the Adam optimizer with a learning rate $lr = 0.001$, no scheduler, batches of size 128, embeddings with 72 dimensions and perturbation value $\gamma = 1$. Moreover, we use $\beta = 0.01$ and we conduct the training for 2000 iterations.
- Permuted MNIST-10 and Permuted MNIST-100 – the hypernetwork and target network used are two-layered MLPs with 100 neurons per layer and 1000 neurons per layer, respectively. We do not use any data augmentation and we choose the Adam optimizer with a learning rate $lr = 0.001$, no scheduler. We use batch size equal to 128, embeddings with 24 dimensions, perturbation value $\gamma = 0.5$, $\beta = 0.01$ and conduct the training for 5000 iterations.
- Split CIFAR-10 – we use a one-layered MLP with 100 neurons as the hypernetwork and AlexNet with batch normalization as the target network. We do not apply any data augmentation. We use the Adam optimizer with a learning rate $lr = 0.001$ and the lr scheduler. We use batch size equal to 128, embeddings with 48 dimensions, perturbation value $\gamma = 0.5$, $\beta = 0.001$ and conduct the training for 2000 iterations.
- Split CIFAR-100 (10 tasks, 10 classes each) – we use a one-layered MLP with 100 neurons as the hypernetwork and ResNet-18 with batch normalization as the target network. We apply the data augmentation as in (Goswami et al. 2024), use the Adam optimizer with a learning rate $lr = 0.001$ and the lr scheduler. We use batch size equal to 32, embeddings with 48 dimensions, perturbation value $\gamma = 1$, $\beta = 0.01$ and conduct the training for 200 epochs.

- Split CIFAR-100 (20 tasks, 5 classes each) – we use a one-layered MLP with 100 neurons as the hypernetwork and AlexNet with batch normalization as the target network. We do not apply any data augmentation, use the Adam optimizer with a learning rate $lr = 0.001$ and the lr scheduler. We use batch size equal to 32, embeddings with 24 dimensions, perturbation value $\gamma = 0.1$, $\beta = 0.01$ and conduct the training for 50 epochs.
- TinyImageNet – we use a one-layered MLP with 200 neurons per layer as the hypernetwork and ResNet-18 with batch normalization as the target network. We apply the data augmentation, use the Adam optimizer with a learning rate $lr = 0.0001$ and the lr scheduler. We use batch size equal to 256, embeddings with 700 dimensions, $\beta = 0.1$ and we conduct the training for 10 epochs. For this dataset, we choose the perturbation value $\gamma = 0.1$.

Unknown task identity hyperparameters – universal embedding In this setting, we use the $\cos(\cdot)$ interval nesting method, as it gave the best performance results. Moreover, there is an additional parameter specifying a custom embedding initialization, which means we initialize the next task’s embedding as the previously learned one. In this setup, we always use the custom embedding initialization. We would like to emphasize that it is just another way of initialization, we do not change or additionally train any of the previously learned embeddings. Let us cover the parameters used in this setting:

- Split MNIST – we use the same hypernetwork and target network architectures as in the previous setup, as well as data augmentation. We apply the Adam optimizer with a learning rate $lr = 0.001$, no scheduler, batches of size 64, embeddings with 24 dimensions and perturbation value $\gamma = 15$. Moreover, we use $\beta = 0.01$ and conduct the training for 2000 iterations.
- Permuted MNIST-10 and Permuted MNIST-100 – we use the same hypernetwork and target network architectures as in the previous setup with no data augmentation. We use the Adam optimizer with a learning rate $lr = 0.001$, no scheduler, batches of size 128, embeddings with 24 dimensions and perturbation value $\gamma = 5$. Moreover, we use $\beta = 0.01$ and conduct the training for 5000 iterations.
- Split CIFAR-10 – we use the same hypernetwork and target network architectures as in the previous setup, with no data augmentation. We use the Adam optimizer with a learning rate $lr = 0.001$ and the lr scheduler. We use batch size equal to 128, embeddings with 48 dimensions, perturbation value $\gamma = 5$, $\beta = 0.01$ and conduct the training for 2000 iterations.
- Split CIFAR-100 (5 tasks, 20 classes per each) – we use the same hypernetwork and target network architectures as in the previous setup, with no data augmentation. We use the Adam optimizer with a learning rate $lr = 0.001$ and the lr scheduler. We use batch size equal to 32, embeddings with 48 dimensions, perturbation value $\gamma = 10$,

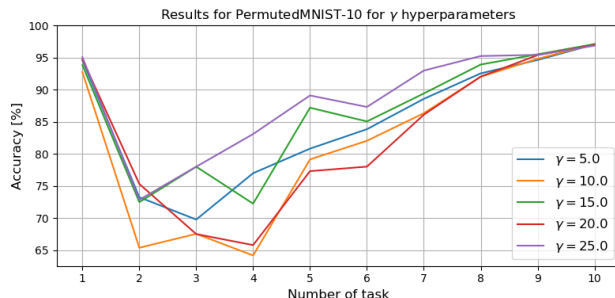
$\beta = 0.01$ and conduct the training for 20 epochs. We use data augmentation.

Unknown task identity hyperparameters – interval entropy In this setup, for each dataset, we use the same best training hyperparameters that were mentioned in the known task identity setting. We test our networks with different perturbation values, thus sometimes obtaining better test results for smaller perturbations γ than the maximal ones seen during training. For Split MNIST we test with $\gamma = 0.0505$, for Permuted MNIST-10 with $\gamma = 0.005$, and for Split CIFAR-100 (5 tasks, 20 classes each) we test with $\gamma = 0.2575$.

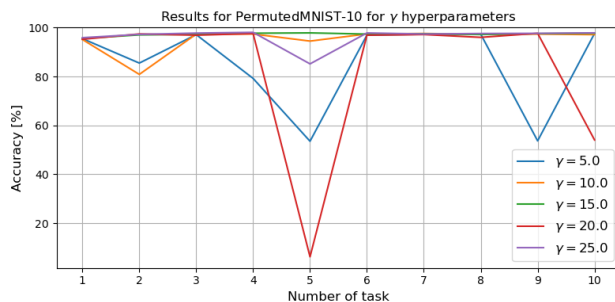
H Ablation study

H.1 Different perturbation size of intervals on Permuted MNIST-10

In this subsection, we experiment with different perturbed values to show that size of the perturbation impacts the ability of our method to find good solutions. As stated in the main section of this work, the larger the perturbation value, the larger the embedding intervals. One could argue that increasing the perturbed value is similar to giving more difficult adversary examples on the input to our network. As pre-



(a) Results obtained using the nesting by the $\cos(\cdot)$ method.



(b) Results obtained for the known task identity setup.

Figure 3: Mean test accuracy for consecutive CL tasks averaged over 2 runs of different interval size settings of HyperInterval for 10 tasks of Permuted MNIST-10 dataset.

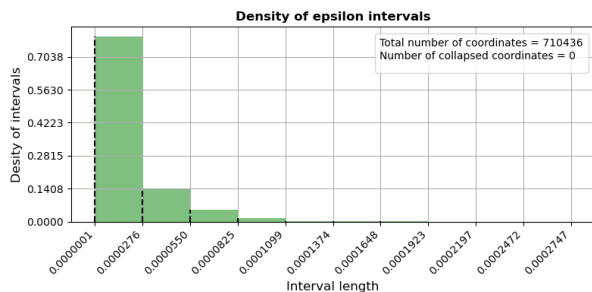
viously mentioned, larger perturbed value on the input embedding intervals implicates an increase in the space where

a universal embedding could be found. Hence, it could make the process of finding an intersection of intervals easier.

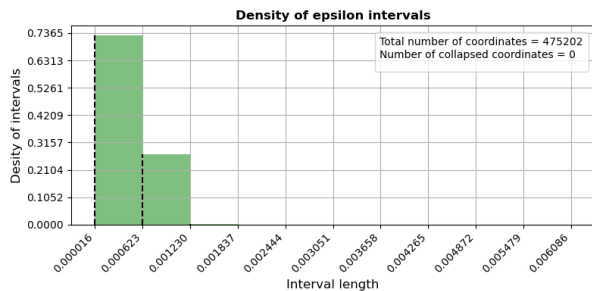
We consider both class and task incremental settings, nesting with the $\cos(\cdot)$ method when applicable. The rest of the parameters are the same as for the best performing models. The grid search outcome is shown in Figure 3. Considering results averaged over 2 runs, the best parameter for the unknown task identity is $\gamma = 25$, while for the known task identity is $\gamma = 15$. These parameters differ from our final choice in Appendix G, since another γ values give better accuracy, based on the averaged results of 5 different runs.

H.2 Interval lengths of target network weights

Using the interval arithmetic within a hypernetwork gives us a possibility of generating interval target network weights. Nevertheless, very often these solutions can become degraded to a point estimate in the network weight space. Since such possibility exists, it is important to check if our hypernetwork generates such output.



(a) Results obtained for the Split CIFAR-100 dataset using the $\cos(\cdot)$ nesting method.



(b) Results obtained for the Split MNIST using the $\cos(\cdot)$ nesting method.

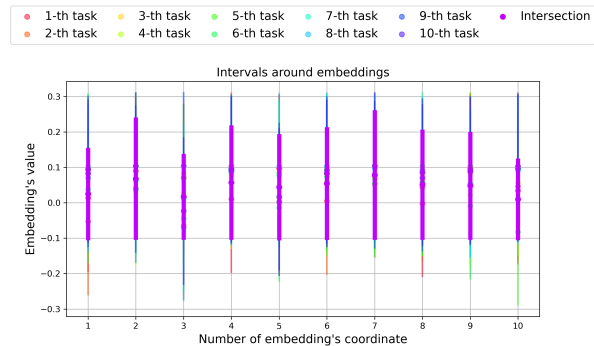
Figure 4: Histograms are calculated for the Split MNIST and Split CIFAR-100 datasets using the MLP and ResNet-18 architectures, respectively.

In Figure 4 we present histogram plots of lengths of target network interval weights to analyse whether this situation occurs. We also give a specific number of coordinates (weights) which collapse to a point for the sake of clarity. We show one result per each type of the target network: an MLP on the Split MNIST dataset and a convolutional network on the Split CIFAR-100 dataset, both with the $\cos(\cdot)$ nesting method. From Figure 4 we may conclude that, for

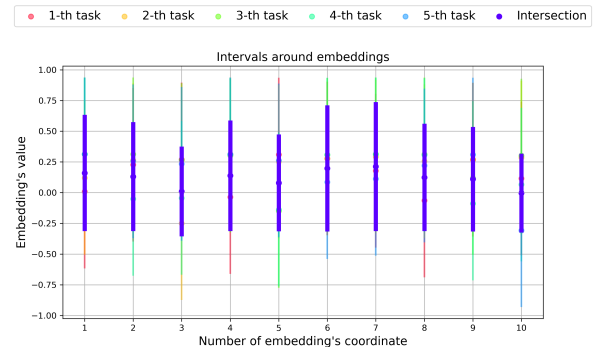
Split CIFAR-100 and Split MNIST, none of the coordinates collapse to a trivial point in the weight space, meaning we obtain non-trivial universal weights.

H.3 Intervals around embeddings – Permuted MNIST-10 and Split MNIST

In this subsection, we present the acquired embedding intervals on the Permuted MNIST-10 and Split MNIST datasets. We use the class incremental setting, where the task identity is unknown and the interval vector is non-learnable (fixed). Results are shown in Figure 5 for nesting with the $\cos(\cdot)$ method.



(a) Results obtained for the Permuted MNIST-10 dataset using the $\cos(\cdot)$ nesting method.



(b) Results obtained for the Split MNIST dataset using the $\cos(\cdot)$ nesting method.

Figure 5: Ten first intervals around task embeddings for Permuted MNIST-10 and Split MNIST.

H.4 Larger number of tasks – Permuted MNIST-100

It is a fair question to ask, how our method performs when there is a larger number of tasks, for example 100 instead of 10. This is a more difficult setting, since the capacity of our model to learn new tasks and remember the previous ones is limited. In such situations, catastrophic forgetting occurs much easier, due to the growing size of knowledge that could be forgotten.

To answer this question, in this section, we provide an analysis of interval arithmetic learning method performance

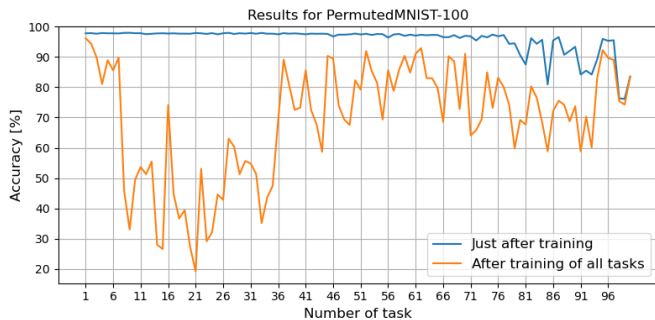


Figure 6: Mean test accuracy for consecutive CL tasks averaged over 3 runs for 100 tasks of Permuted MNIST–100 dataset.

given the Permuted MNIST-100 dataset. As a reminder, this dataset consists of 100 tasks comparing pairs of images of numbers subjected to different distortions. Due to the number of tasks and the size of the dataset, we limit ourselves to provide results for the task incremental setting, with learnable interval parameters and no nesting.

The results are presented in Figure 6. We observe that training on consecutive tasks has a significant impact on the accuracy on previously learned tasks. Nevertheless, our model is still able to retain some of the previous knowledge, not dropping to a random accuracy on any of the tasks. Furthermore, we conclude that training consecutive tasks in the latter stages is more difficult, due to the decrease in accuracy just after training.

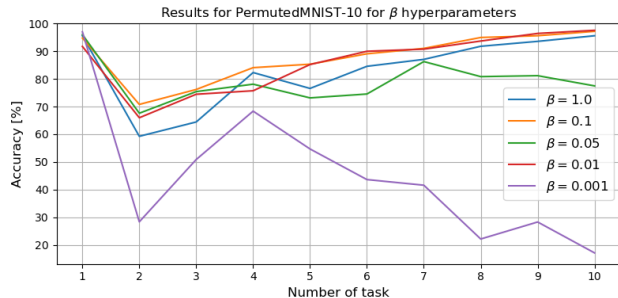
H.5 Ablation of the regularization method

This subsection involves experimenting with different values for the β parameter, which directly impacts the memorization factor in the loss function. This part of mathematical expression targets specifically the hypernetwork output. The experiment is done in two setups: 1) task incremental learning, 2) class incremental learning. We conduct a grid search on the Permuted MNIST-10 dataset and check the β parameter from a set of values: $\{1.0, 0.1, 0.05, 0.01, 0.001\}$, while the rest of parameters are taken from the best performing models. The grid search results are presented in Figure 7.

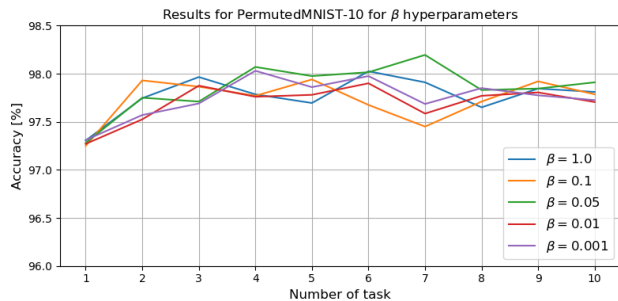
It is important to emphasize that the larger the β parameter, the stronger the regularization of knowledge learned on the previous tasks. This implies that we put more stress on our model to remember previous tasks and limit its ability to learn a new one. Based on the results averaged over two runs, the best parameters are $\beta = 0.1$ for the CIL setup and $\beta = 0.05$ for the TIL setup. However, these parameters differ from our final choice in Appendix G, since the parameter value $\beta = 0.01$ gives better accuracy scores for both setups, based on the averaged results of 5 different runs.

H.6 Different interval nesting methods

In this experimental subsection, we focus on the comparison of two different approaches to interval nesting of the input embedding to the hypernetwork. We experiment on



(a) Results obtained in the class incremental setting, using the nesting by the $\cos(\cdot)$ method.



(b) Results obtained in the task incremental setting.

Figure 7: Mean test accuracy for consecutive CL tasks averaged over 2 runs with different β hyperparameters of HyperInterval for 10 tasks of Permuted MNIST-10 dataset.

Permuted MNIST-10 and consider two interval mappings: $\tanh(\cdot)$ and $\cos(\cdot)$. The results are shown in Figure 8. We may conclude that intervals obtained with $\tanh(\cdot)$ and $\cos(\cdot)$ behave similarly, especially on the final tasks.

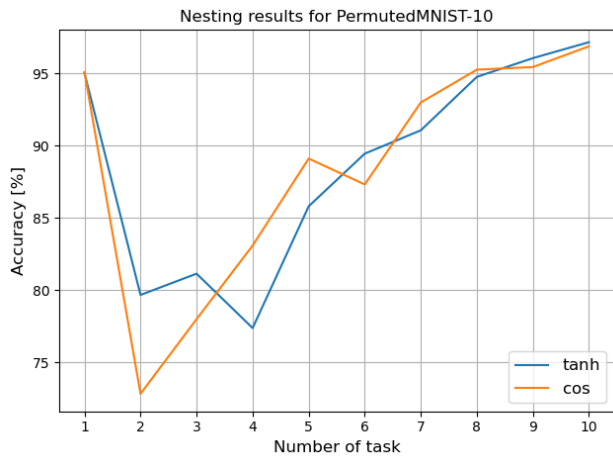


Figure 8: Mean test accuracy for consecutive continual learning (CL) tasks averaged over 2 runs using $\tanh(\cdot)$ and $\cos(\cdot)$ nesting methods for 10 tasks on the Permuted MNIST-10 dataset.

Both $\cos(\cdot)$ and $\tanh(\cdot)$ mappings have this in common, that they scale every coordinate of the task embedding interval to be in range $[-1, 1]$. These functions also guarantee we find a non-empty intersection of task embeddings, when we multiply each coordinate by a factor of $\frac{\gamma}{M}$, where γ is the perturbation value and M is the embedding dimension. Hence there exists a universal embedding, in the worst case being a trivial point in the embedding space.

I Additional experimental results

Task incremental learning Results for accuracy behaviour before and after training on consecutive tasks on TinyImageNet are shown in Figure 11. Generally, the accuracy after training on all tasks is comparable to the accuracy obtained just after training on the specific task. This shows lack of catastrophic forgetting when dealing with a bigger number of tasks. Figure 12 shows detailed test accuracy scores after training on consecutive tasks. We can observe small decrease in accuracy on previous tasks and overall consistency in predictions. In Figure 9, the 95% confidence intervals are shown with the mean test accuracy for each task, averaged over 5 different runs. In case of Permuted MNIST, the average test accuracy before and after training on consecutive tasks behaves similarly. Moreover, the confidence intervals overlap each other.

Class incremental learning Confidence interval plots for unknown task identity are shown in Figure 10. Firstly, we observe that on Split CIFAR-100, our model is able to learn the first task but has difficulties with learning consecutive tasks. It might be because Split CIFAR-100 is too difficult

to solve with one universal embedding. Secondly, large standard deviations on Split MNIST show that the HyperInterval training on this dataset is unstable, especially visible in accuracy on the initial tasks after learning on all tasks. Specific test accuracy scores for Permuted MNIST-10 and Split MNIST, on each consecutive task, are shown in Figure 13. We observe positive backward transfer for the second task of Split MNIST and high accuracy values on the diagonal for Permuted MNIST-10, corresponding to the accuracy just after training on the specific task. On the right-hand side of Figure 9 we show that HyperInterval can learn new tasks with high accuracy just after training for Permuted MNIST-10.

I.1 Time complexity

In this subsection, we present the training times for HyperInterval using the following datasets and graphics cards: 1) PermutedMNIST (DGX); 2) SplitMNIST (RTX 4090), TinyImageNet (RTX 4090), and CIFAR-100 (RTX 4090). The detailed results are shown in Table 4. We report the training times for two scenarios: TIL and CIL. It is crucial to distinguish between these two scenarios because their training procedures differ.

PermutedMNIST and SplitMNIST are datasets on which HyperInterval was trained in both TIL and CIL scenarios simultaneously. The results indicate that HyperInterval’s training duration is approximately 35 minutes longer for PermutedMNIST in the CIL scenario compared to the TIL scenario. In the case of the SplitMNIST dataset, the training times are nearly identical for both scenarios. Notably, the longest training duration for HyperInterval is observed with the CIFAR-100 dataset (10 tasks, 10 classes per task). This extended duration can be attributed to the challenges involved in training interval convolutional layers to achieve satisfactory performance. These layers typically require more training steps to ensure a gradual increase in interval length. Additionally, a small batch size was used.

References

Aljundi, R.; Babiloni, F.; Elhoseiny, M.; Rohrbach, M.; and Tuytelaars, T. 2018. Memory Aware Synapses: Learning what (not) to forget. In *Proceedings of the European Conference on Computer Vision (ECCV)*.

Aljundi, R.; Belilovsky, E.; Tuytelaars, T.; Charlin, L.; Caccia, M.; Lin, M.; and Page-Caccia, L. 2019. Online continual learning with maximal interfered retrieval. In *Advances in Neural Information Processing Systems (NeurIPS)*, volume 32. Curran Associates, Inc.

Belouadah, E.; and Popescu, A. 2019. IL2M: Class incremental learning with dual memory. In *International Conference on Computer Vision (ICCV)*.

Castro, F. M.; Marín-Jiménez, M. J.; Guil, N.; Schmid, C.; and Alahari, K. 2018. End-to-end incremental learning. In *European Conference on Computer Vision (ECCV)*.

Chaudhry, A.; Dokania, P. K.; Ajanthan, T.; and Torr, P. H. 2018. Riemannian walk for incremental learning: Understanding forgetting and intransigence. In *Proceedings of the European conference on computer vision (ECCV)*, 532–547.

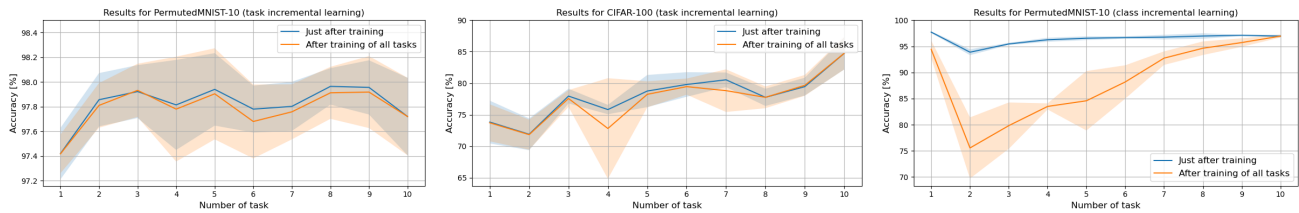
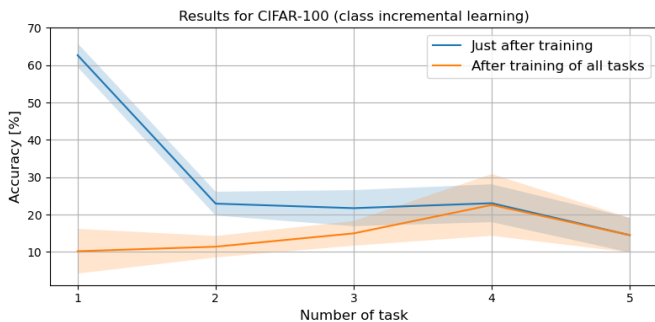


Figure 9: Average test accuracy (with 95% confidence intervals) for Permuted MNIST-10 for 10 tasks and Split CIFAR-100 for 10 tasks.

Table 4: Mean time complexity averaged over 5 seeds with standard deviations for HyperInterval in the format HH:MM:SS.

| Dataset Name | TIL | | CIL | |
|---------------------------------------|----------|----------|----------|----------|
| PermutedMNIST | 01:11:17 | 00:00:27 | 01:47:56 | 00:00:21 |
| SplitMNIST | 00:07:29 | 00:00:11 | 00:07:39 | 00:00:13 |
| TinyImageNet | 00:57:37 | 00:01:32 | - | - |
| CIFAR-100 (10 tasks, 10 classes each) | 06:24:50 | 00:07:18 | - | - |
| CIFAR-100 (5 tasks, 20 classes each) | - | - | 02:47:26 | 00:10:48 |



(a) Results obtained using the nesting by the $\cos(\cdot)$ method.



(b) Results obtained using the nesting by the $\cos(\cdot)$ method.

Figure 10: Average test accuracy (with 95% confidence intervals) for Split CIFAR-100 and Split MNIST for 5 tasks. Results are obtained using the $\cos(\cdot)$ nesting method.

Cywiński, B.; Deja, K.; Trzciński, T.; Twardowski, B.; and Łukasz Kuciński. 2024. GUIDE: Guidance-based Incremental Learning with Diffusion Models. *ArXiv:2403.03938*.

Dahlquist, G.; and Björck, Å. 2008. *Numerical methods in scientific computing, volume I*. SIAM.

Deng, Z.; and Russakovsky, O. 2022. Remember the past: Distilling datasets into addressable memories for neural networks. In *Advances in Neural Information Processing Systems (NeurIPS)*, volume 35, 34391–34404.

French, R. M. 1999. Catastrophic forgetting in connectionist networks. *Trends in cognitive sciences*, 3(4): 128–135.

Goswami, D.; Liu, Y.; Twardowski, B.; and van de Weijer, J. 2024. FeCAM: Exploiting the Heterogeneity of Class Distributions in Exemplar-Free Continual Learning. *arXiv:2309.14062*.

Gowal, S.; Dvijotham, K.; Stanforth, R.; Bunel, R.; Qin, C.; Uesato, J.; Arandjelovic, R.; Mann, T.; and Kohli, P. 2018. On the effectiveness of interval bound propagation for training verifiably robust models. *arXiv preprint arXiv:1810.12715*.

Ha, D.; Dai, A.; and Le, Q. V. 2016. Hypernetworks. *arXiv preprint arXiv:1609.09106*.

Henning, C.; Cervera, M.; D’Angelo, F.; Von Oswald, J.; Traber, R.; Ehret, B.; Kobayashi, S.; Grewe, B. F.; and Sacramento, J. 2021. Posterior meta-replay for continual learning. *Advances in Neural Information Processing Systems*, 34: 14135–14149.

Hou, S.; Pan, X.; Loy, C. C.; Wang, Z.; and Lin, D. 2019. Learning a unified classifier incrementally via rebalancing. In *International Conference on Computer Vision (ICCV)*.

Kang, H.; Yoon, J.; Madjid, S. R.; Hwang, S. J.; and Yoo, C. D. 2023. Forget-free Continual Learning with Soft-Winning SubNetworks. *arXiv:2303.14962*.

Kirkpatrick, J.; Pascanu, R.; Rabinowitz, N.; Veness, J.; Desjardins, G.; Rusu, A. A.; Milan, K.; Quan, J.; Ramalho, T.;

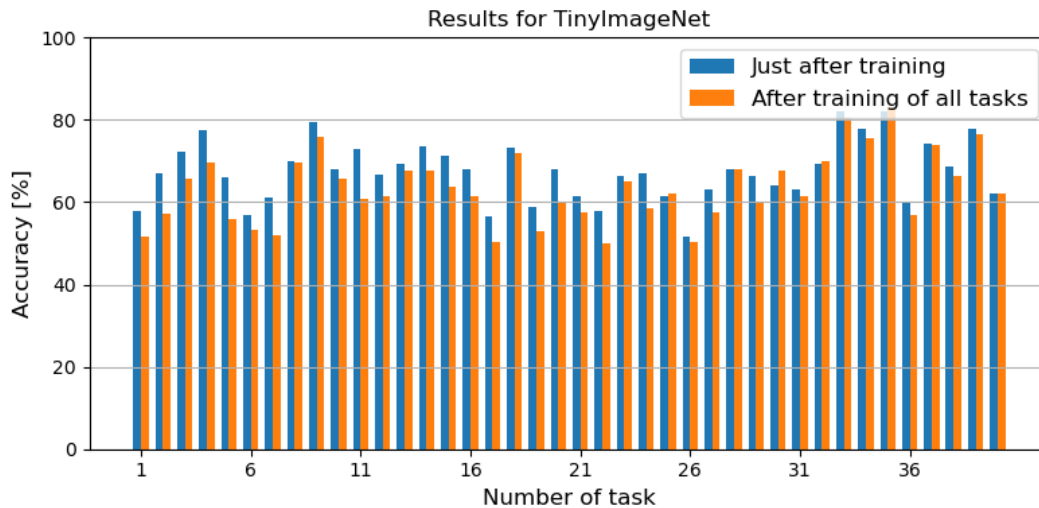


Figure 11: Test accuracy of HyperInterval for each task of TinyImageNet. We select one model trained on all 40 tasks, in the known task identity setup.

Grabska-Barwinska, A.; et al. 2017. Overcoming catastrophic forgetting in neural networks. *Proceedings of the National Academy of Sciences*, 114(13): 3521–3526.

Książek, K.; and Spurek, P. 2023. HyperMask: Adaptive Hypernetwork-based Masks for Continual Learning. *arXiv preprint arXiv:2310.00113*.

Lee, K. H. 2004. *First course on fuzzy theory and applications*, volume 27. Springer Science & Business Media.

Li, Z.; and Hoiem, D. 2017. Learning without forgetting. *IEEE transactions on pattern analysis and machine intelligence*, 40(12): 2935–2947.

Liu, Y.; Liu, A.-A.; Su, Y.; Schiele, B.; and Sun, Q. 2020. Mnemonics training: Multi-class incremental learning without forgetting. In *Computer Vision and Pattern Recognition (CVPR)*.

Lopez-Paz, D.; and Ranzato, M. 2017. Gradient Episodic Memory for Continual Learning. In *Proceedings of the Advances in Neural Information Processing Systems (NeurIPS)*.

Mallya, A.; Davis, D.; and Lazebnik, S. 2018. Piggyback: Adapting a Single Network to Multiple Tasks by Learning to Mask Weights. In *Proceedings of the European Conference on Computer Vision (ECCV)*.

Mallya, A.; and Lazebnik, S. 2018. Packnet: Adding multiple tasks to a single network by iterative pruning. In *Proceedings of the IEEE Conference on Computer Vision and Pattern Recognition (CVPR)*.

Masse, N. Y.; Grant, G. D.; and Freedman, D. J. 2018. Alleviating catastrophic forgetting using context-dependent gating and synaptic stabilization. *Proceedings of the National Academy of Sciences*, 115: E10467 – E10475.

McCloskey, M.; and Cohen, N. J. 1989. Catastrophic interference in connectionist networks: The sequential learning

problem. In *Psychology of learning and motivation*, volume 24, 109–165. Elsevier.

Nguyen, C. V.; Li, Y.; Bui, T. D.; and Turner, R. E. 2018. Variational continual learning. In *International Conference on Learning Representations (ICLR)*.

Prabhu, A.; Torr, P. H.; and Dokania, P. K. 2020. Gdumb: A simple approach that questions our progress in continual learning. In *Proceedings of the European Conference on Computer Vision (ECCV)*, 524–540.

Ratcliff, R. 1990. Connectionist models of recognition memory: constraints imposed by learning and forgetting functions. *Psychological review*, 97(2): 285.

Rebuffi, S.; Kolesnikov, A.; Sperl, G.; and Lampert, C. H. 2017. iCaRL: Incremental Classifier and Representation Learning. In *Computer Vision and Pattern Recognition (CVPR)*.

Rolnick, D.; Ahuja, A.; Schwarz, J.; Lillicrap, T. P.; and Wayne, G. 2019. Experience Replay for Continual Learning. In *Proceedings of the Advances in Neural Information Processing Systems (NeurIPS)*.

Rostami, M.; Kolouri, S.; and Pilly, P. K. 2019. Complementary learning for overcoming catastrophic forgetting using experience replay. In *International Joint Conference on Artificial Intelligence (IJCAI)*, 3339–3345.

Russakovsky, O.; Deng, J.; Su, H.; Krause, J.; Satheesh, S.; Ma, S.; Huang, Z.; Karpathy, A.; Khosla, A.; Bernstein, M.; Berg, A. C.; and Fei-Fei, L. 2015. ImageNet Large Scale Visual Recognition Challenge. *arXiv:1409.0575*.

Rusu, A. A.; Rabinowitz, N. C.; Desjardins, G.; Soyer, H.; Kirkpatrick, J.; Kavukcuoglu, K.; Pascanu, R.; and Hadsell, R. 2016. Progressive neural networks. *arXiv preprint arXiv:1606.04671*.

Shin, H.; Lee, J. K.; Kim, J.; and Kim, J. 2017. Continual Learning with Deep Generative Replay. In *Proceedings*

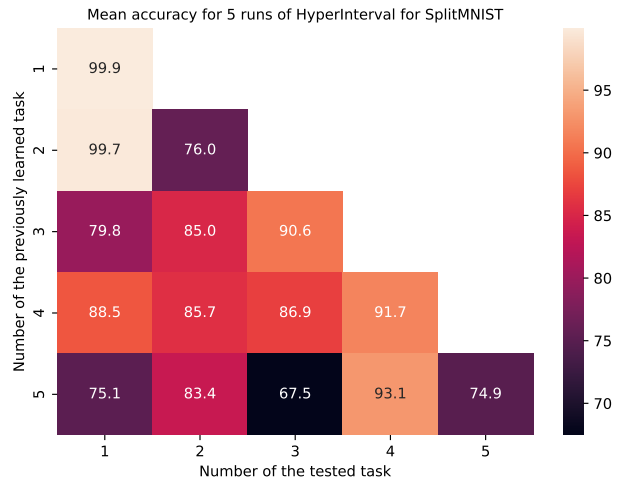
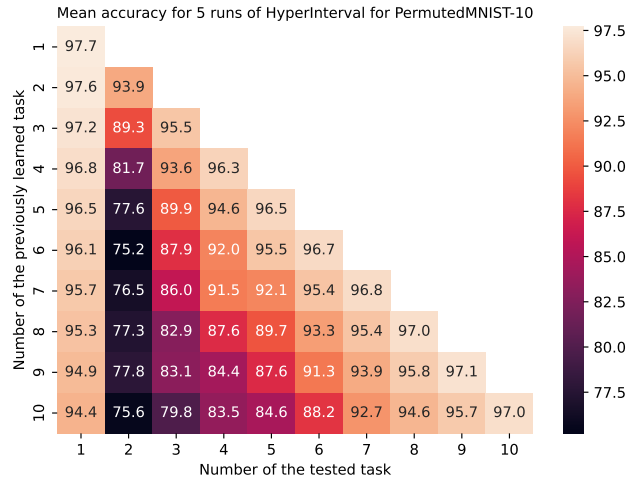
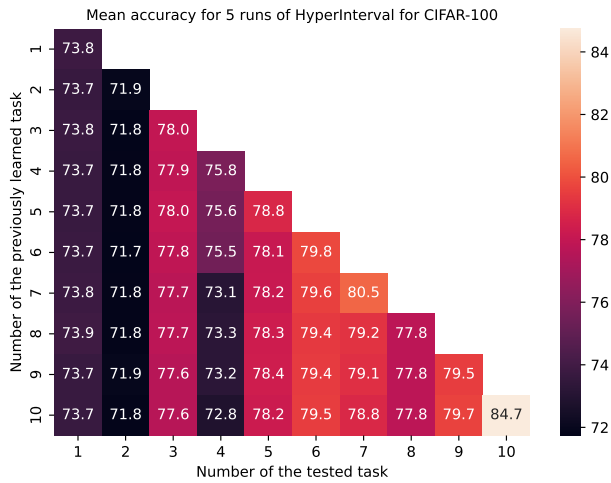
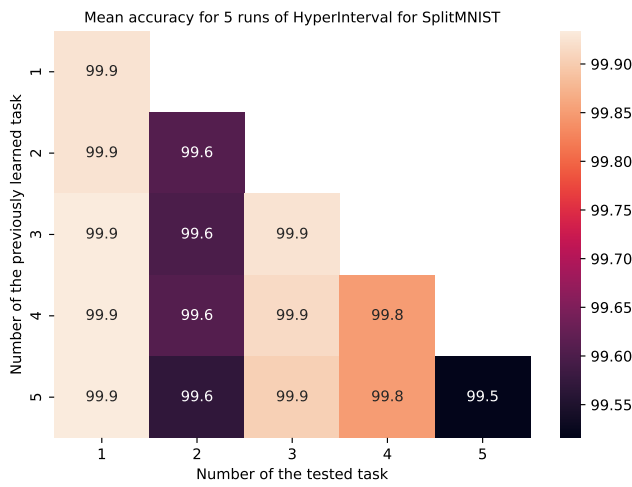
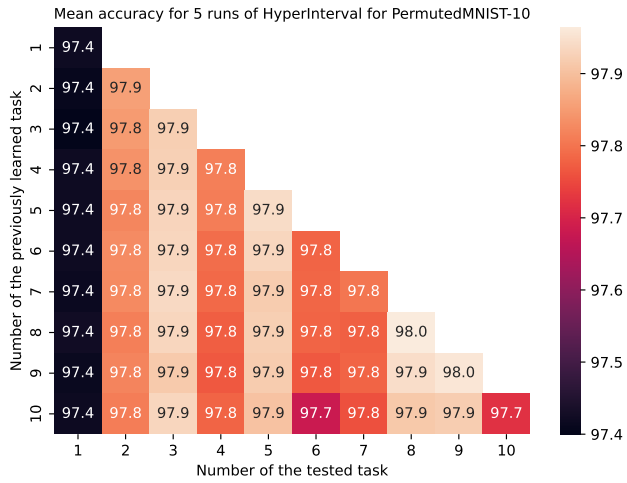


Figure 13: Mean test accuracy for consecutive CL tasks averaged over five runs of the best models. Results are obtained with the $\cos(\cdot)$ nesting method.

Figure 12: Mean test accuracy for consecutive CL tasks averaged over five runs of the best models. Results are obtained for the known task identity setup. The diagonal corresponds to testing the task just after the model was trained on it. The sub-diagonal values correspond to testing the task after the model was trained on consecutive tasks.

of the *Advances in Neural Information Processing Systems (NeurIPS)*.

van de Ven, G. M.; Siegelmann, H. T.; and Tolias, A. S. 2020. Brain-inspired replay for continual learning with artificial neural networks. *Nature Communications*, 11.

van de Ven, G. M.; and Tolias, A. S. 2018. Generative replay with feedback connections as a general strategy for continual learning. ArXiv:1809.10635.

van de Ven, G. M.; and Tolias, A. S. 2019. Three scenarios for continual learning. ArXiv:1904.07734.

Virmaux, A.; and Scaman, K. 2018. Lipschitz regularity of deep neural networks: analysis and efficient estimation. In Bengio, S.; Wallach, H.; Larochelle, H.; Grauman, K.; Cesa-Bianchi, N.; and Garnett, R., eds., *Advances in Neural Information Processing Systems*, volume 31. Curran Associates, Inc.

von Oswald, J.; Henning, C.; Grewe, B. F.; and Sacramento, J. 2019. Continual learning with hypernetworks. In *International Conference on Learning Representations*.

von Oswald, J.; Henning, C.; Grewe, B. F.; and Sacramento, J. 2020. Continual learning with hypernetworks. In *International Conference on Learning Representations*.

Wang, T.; Zhu, J.-Y.; Torralba, A.; and Efros, A. A. 2018. Dataset distillation. ArXiv:1811.10959.

Wołczyk, M.; Piczak, K.; Wójcik, B.; Pustelnik, L.; Morawiecki, P.; Tabor, J.; Trzcinski, T.; and Spurek, P. 2022. Continual learning with guarantees via weight interval constraints. In *International Conference on Machine Learning*, 23897–23911. PMLR.

Wortsman, M.; Ramanujan, V.; Liu, R.; Kembhavi, A.; Rastegari, M.; Yosinski, J.; and Farhadi, A. 2020. Supermasks in superposition. In *Neural Information Processing Systems (NeurIPS)*, 15173–15184.

Wu, Y.; Chen, Y.; Wang, L.; Ye, Y.; Liu, Z.; Guo, Y.; and Fu, Y. 2019. Large scale incremental learning. In *International Conference on Computer Vision (ICCV)*.

Yoon, J.; Yang, E.; Lee, J.; and Hwang, S. J. 2018. Lifelong Learning with Dynamically Expandable Networks. In *International Conference on Learning Representations (ICLR)*.

Zenke, F.; Poole, B.; and Ganguli, S. 2017. Continual learning through synaptic intelligence. In *International Conference on Machine Learning (ICML)*, 3987–3995.

Zhao, B.; Mopuri, K. R.; and Bilen, H. 2021. Dataset condensation with gradient matching. In *International Conference on Learning Representations (ICLR)*.